

The normal phase of quasi-one-dimensional organic superconductors

C. Bourbonnais and D. Jérôme^a

*Centre de Recherche en Physique du Solide et Département de Physique
Université de Sherbrooke, Sherbrooke, Québec, Canada J1K 2R1.*

^a *Laboratoire de Physique des Solides, associé au CNRS, Bâtiment 510
Université de Paris-sud, 91405 Orsay, France*

Abstract

We review the properties of quasi-one-dimensional organic superconductors: the Bechgaard salts and their sulfur analogs in their normal phase precursor to long-range order. We go through the main observations made in the normal state of these systems at low magnetic field and tackle the issue of their description under the angles of the Fermi and Luttinger liquid pictures.

1. Introduction

The quest for superconductivity at always higher temperature has been a constant motivation in the material science research over the past quarter of the century. A well known example is the huge amount of work which has been invested in the synthesis, measurements and processing of intermetallic compounds belonging to the A-15 family of type II superconductors. These compounds V_3Si [1] and Nb_3Sn [2] are still at present the materials mostly used when superconductivity comes to applications [3].

In the meantime some new routes towards high temperature and possibly exotic superconductivity have been investigated. This is the case for the heavy fermion compounds in which the close interplay between local magnetic moments and the spin of delocalized electrons has led to the possibility of a non-phonon mediated mechanism for electron pairing [4]. A very successful route towards high- T_c 's has been followed with conducting layered cuprates after the discovery of superconductivity in $(La, Sr)_2CuO_4$ [5].

More exotic has been the proposal made by Little for the possibility of an excitonic pairing mechanism in some organic conductors leading to a supposedly tremendously large increase of T_c [6]. Little's mechanism relies on the possibility to obtain an attractive interaction between the mates of a Cooper pair in an energy range extending up to the Fermi energy (i.e. 10,000 K) instead of the limited range imposed by the phonon energy (100-300 K) in the well-known BCS mechanism of conventional superconductivity [7]. A prerequisite to Little's mechanism was the synthesis of a conducting molecular backbone with highly polarizable branched molecules. Unfortunately – or possibly fortunately – a lot of physics problems had been overlooked in the suggestion of W. Little. Molecular conduction requires the existence of chemically stable open shell molecules able to provide

charges likely to delocalize via intermolecular overlap. A first attempt has been reported in 1954 in perylene oxidized with bromine [8]. However, this conducting salt failed to present the desired stability. Two tracks have been followed for the synthesis of stable organic conductors. The first successful try has been obtained by forming a compound with molecules of two different chemical nature: one molecule that can be easily oxidized in the presence of another one which is reduced giving rise to a charge transfer complex. A prototype for such a system is the charge transfer compound tetrathiafulvalene-tetracyanoquinodimethane (TTF-TCNQ), that contains both anion (TCNQ) and cation (TTF) in the ratio 1:1 [9, 10]. The planar molecules of TTF-TCNQ form segregated stacks in a plane to plane manner and the molecular (p-type) orbitals can interact preferentially along the stacking direction.

In spite of the interstack interaction occurring mainly between TTF and TCNQ stacks through S-N contacts, the dispersion of energy which derives from the intermolecular overlap is one dimensional i.e., the dispersion is governed only by the longitudinal wave vector giving rise to a flat Fermi surface which is the signature of a 1-D conductor. The symmetry of the molecular orbitals and the molecular stacking is responsible for a band structure consisting of two inverted conduction band intersecting at the single Fermi wave vector $\pm k_F^0$ related to the charged r transferred from neutral TTF to neutral TCNQ by $2k_F^0 = (\pi/a)r$, where a is the unit cell length along the stacking direction. The room conductivity of TTF-TCNQ is large, $\sigma \sim 500 (\Omega \cdot \text{cm})^{-1}$ [11, 12] and increases even more at lower temperature reaching $10^4 (\Omega \cdot \text{cm})^{-1}$ at 60 K – although much higher values have been claimed by Heeger and co-workers [9]. However, the dramatic increase of the conductivity breaks down at 54 K while a transition towards an insulating ground state takes

place. Diffuse X-ray scattering experiments [13] have shown that the 54 K metal-insulator transition can be related to the instability of a 1-D electron gas which had been proposed earlier by Peierls [14]. Attempts to suppress the Peierls state and stabilize a conducting (and possibly superconducting state) by increasing the 3-D character of the 1-D conductor [15] proved to be unsuccessful since the Peierls transition is raised from 54 to 72 K under 35 kbar [16]. In spite of this failure, high-pressure studies have shown a steady increase of the charge transfer with a commensurability regime in the 14-19 kbar pressure domain ($r = 2/3$ or $2k_F^0 = 2\pi/3a$) (Figure 1) [17, 18].

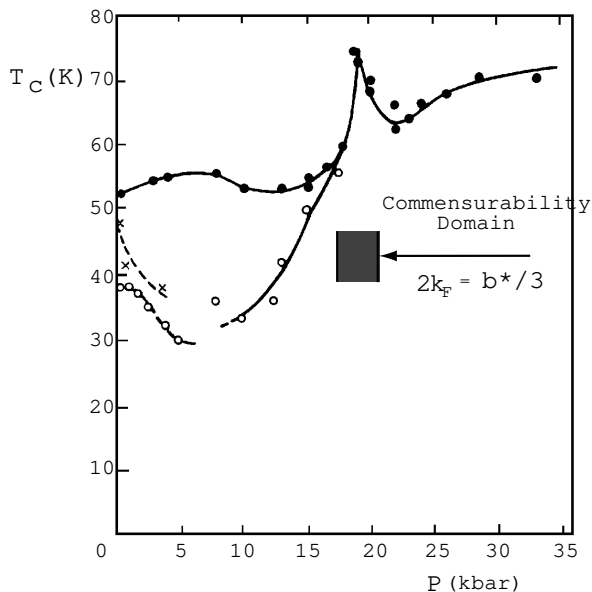


Figure 1: Phase diagram of TTF-TCNQ derived by transport properties measurements, after [17, 18].

However the elaboration of a new charge-transfer conductor, TMTSF-DMTCNQ, and the use of high pressure have provided a clue for the discovery of superconductivity. In TMTSF-DMTCNQ, the TMTSF stacks arrange in sheets where the dominant interchain contact is now between TMTSF stacks. Furthermore the methyl groups in DMTCNQ molecules acting as space fillers weaken the interaction between DMTCNQ along the stacks. Therefore this compound can be described as an organic conductor made of only one type of stacks (the donor stack) [19]. The interest for this compound has been stimulated by the high pressure investigation showing for the first time the possibility to stabilize a highly conducting state ($\sigma \sim 10^4$ ($\Omega \cdot \text{cm}$)⁻¹) at low temperature (Figure 2) [20].

Given the carrier density (0.5 hole/molecule) determined from X-ray diffuse scattering data [21], the effective one-chain character of TMTSF-DMTCNQ and the existence of a weak $4k_F^0$ potential coming from the packing of the DMTCNQ molecules, a new series of one-chain organic salts (TMTSF)₂X, where X is an inorganic monoanion has been synthesized [22] – this latter family, being isostructural with the sulfur series (TMTTF)₂X [23] (Figure 3).

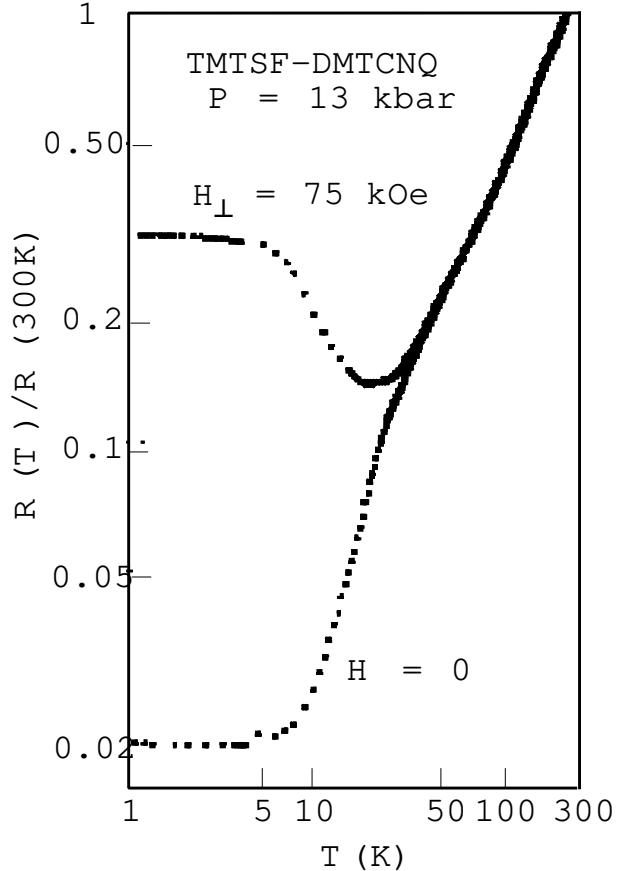


Figure 2: Temperature dependence of the longitudinal resistivity of TMTSF-DMTCNQ under 13 kbar in zero magnetic field and in a transverse field of 75 kOe, after [20].

The possibility to vary the parameters governing the physical properties of (TM)₂X compounds (nature of cation or anion, pressure and application of a magnetic field) allows an exploration moving continuously from half-filled band 1-D Mott insulators in sulfur based compounds to conducting systems in selenium or strongly pressurized sulfur based compounds (Figure 4).

One of the first compounds of the (TM)₂X series to be synthesized has been (TMTTF)₂PF₆ [24], prior to the discovery of the Bechgaard salt (TMTSF)₂PF₆ and this salt did not raise much enthusiasm in the early seventies because of the localized character of the conduction below room temperature instead of the expected metallic behavior [25]. However this compound gained much interest in time since it is the member in the (TM)₂X family which spans the broadest variety of physical properties while changing the pressure [26]. At low pressure, members of the sulfur series can develop either spin-Peierls or commensurate-localized antiferromagnetic long-range order, while either itinerant antiferromagnetism or superconductivity are found in the selenide series. Under pressure the properties of the sulfur series evolves toward those of the selenides.

A large number of theoretical works have been devoted to evaluate the importance of Coulomb interaction in the description of the normal state of the Bechgaard salts.

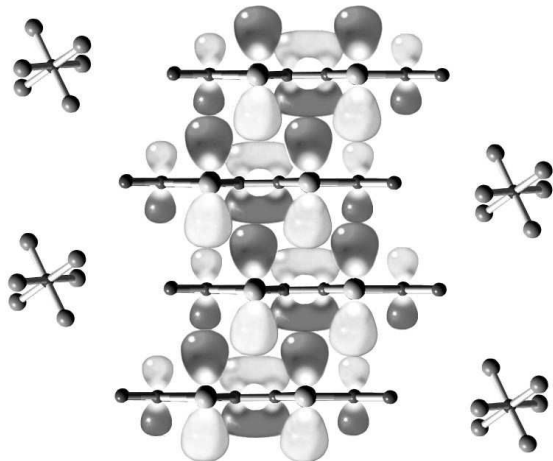


Figure 3: A side view of the $(\text{TM})_2\text{X}$ crystal structure with the electron orbitals of the organic stack. Courtesy of J. Ch. Ricquier.

At the very outset, that these systems show in several circumstances long range antiferromagnetic ordering at sufficiently low temperature does indicate that repulsive interaction among carriers is important. Although a rather large consensus quickly emerged about the relevance of short-range Coulomb interactions in these systems, opinions differ, however, as to the size of these interactions relative to the bandwidth and their role when the temperature is raised outside the critical domain linked to a phase transition and where the system enters in normal state. The reason essentially fits in the fact that the band structure of these systems is characterized by one-electron transfer integrals t_a along the chains which are at least one order magnitude larger than the corresponding integrals t_\perp in the transverse directions making them close realizations of one-dimensional systems. In a one-dimensional metal, interactions have very special if not dramatic consequences on the nature of the electronic state, which turns out to be quite different to what we are used to expect in ordinary metals in three dimensions. In metals, like Cu, Al, ... for example, the Pauli principle considerably restricts the possibility of scattering events in the proximity of the Fermi sphere so the Coulomb repulsion, though strong in amplitude, has very little effect on low-energy carriers which behave as effective free particles, called ‘quasi-particles’. At the heart of the celebrated *Fermi liquid* (FL) theory of the electron state, the concept of quasi-particles proved to be inapplicable when carriers are forced to move and interact within a one-dimensional world. In their linear motion, electrons can hardly avoid each other and the influence of interactions becomes magnified to such an extent that quasi-particles are completely absent from the low-energy excitation spectrum. This occurs to the benefit of spin and charge collective modes which form a distinct electronic state called a *Luttinger liquid* (LL) [27].

It follows that the evaluation of the extent to which one-dimensional physics is relevant has always played an

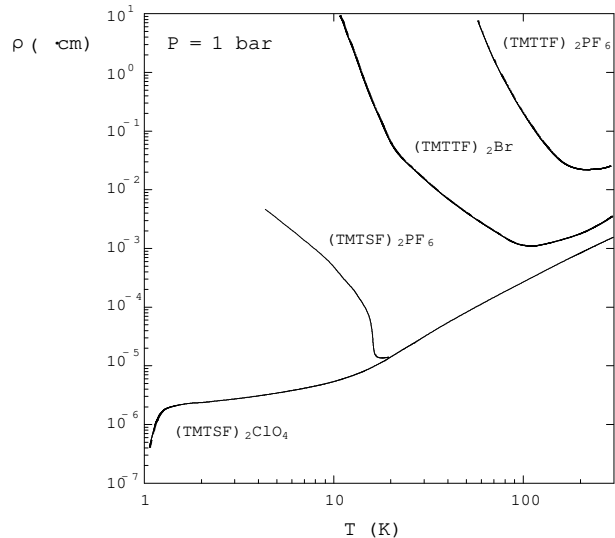


Figure 4: The temperature dependence of the longitudinal resistivities for representatives of $(\text{TM})_2\text{X}$ series.

important part in the debate surrounding the theoretical description of the normal state of these materials. One point of view expressed is that the amplitude of t_\perp in the b direction is large enough for a FL component to develop in the ab plane, thereby governing most properties of the normal phase attainable below say room temperature. In this scenario, the anisotropic Fermi liquid then constitutes the basic electronic state from which various instabilities of the metallic state, like spin-density-wave, superconductivity, etc., arise [29]. Following the example of the BCS theory of superconductivity in conventional superconductors, it is the critical domain of the transition that ultimately limits the validity of the Fermi liquid picture in the low temperature domain.

Another view is to consider the Bechgaard salts as more correlated systems as a result of one-dimensional physics which maintains relevance within a large extent of the normal phase and even affects the mechanisms by which long-range order is stabilized in these materials.

The literature devoted to both experimental and theoretical aspects of $(\text{TM})_2\text{X}$ over the past eighteen years or so, is far too vast to be presented from the top to the bottom within the present short review. A selected interest will thus be put on the nature of the normal phase of the $(\text{TM})_2\text{X}$ compounds. This issue has actually a long history which traces back to the discovery of organic superconductivity and to the first attempts to figure out the origin of this phase in these compounds [30]. It was later on tied with the more general frame of the physics of the normal phase in strongly correlated anisotropic superconductors including high- T_c cuprates. Even within this restricted scope we will not dwell on the particular behavior of the normal phase taking place at low temperature under magnetic field. We refer the reader to recent references on various aspects of anomalous magnetotransport in the $(\text{TM})_2\text{X}$ (see for example [31, 32, 33, 34, 35]).

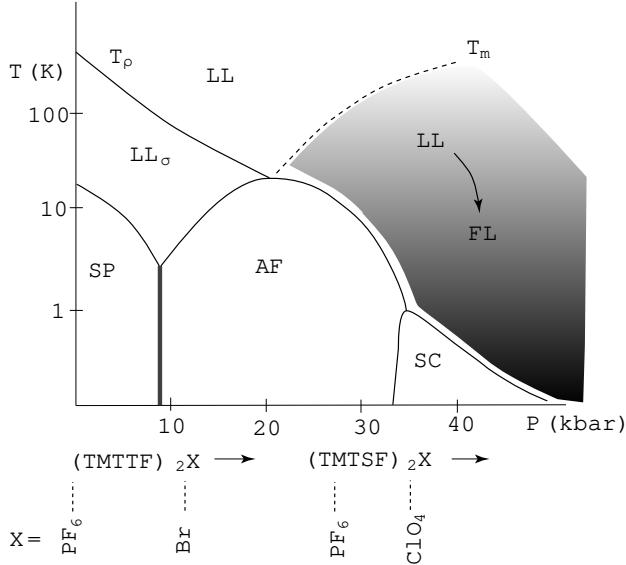


Figure 5: The generic phase diagram of the $(\text{TM})_2\text{X}$ as a function of pressure or anion substitution. On the left, the normal phase of sulfur compounds can be described as a Luttinger liquid that becomes gapped in the charge sector (LL_σ) below T_p and can develop either a spin-Peierls (SP) or localized antiferromagnetic ordered state. Under pressure, the properties of the sulfur series evolve toward those of the selenides for which the normal state shows a progressive restoration of a Fermi liquid (FL) precursor to antiferromagnetism (AF) and superconductivity (S), after [28].

2. Single-particle band theory

The metallic character of the organic conductors to be discussed in this article occurs through the delocalization of unpaired carriers via the overlap of π -orbitals between neighboring molecules (Figure 3). The organic salts of the $(\text{TM})_2\text{X}$ family represent archetypes of 1-D conductors where TM is usually tetramethyltetraselenafulvalene TMTSF, a flat molecule that donates electrons easily and X is a monovalent anion, which either consists of symmetric (PF_6 , AsF_6 , etc.) or asymmetric (ClO_4 , ReO_4 , NO_3 , FSO_3 , SCN , etc.) inorganic molecules.

What is remarkable with the $(\text{TM})_2\text{X}$ series is the variety of different physical situations that can be achieved while changing the chemical nature of the organic donor, i.e. using tetramethylthiafulvalene TMTTF, the sulfur analog of TMTSF that contains four sulfur atoms instead of selenium atoms, changing the nature of the anion (its size or symmetry), synthesizing sulfur-selenium hybrid donors or even ordered (or disordered) solid solutions of TMTTF and TMTSF molecules [36]. All above mentioned compounds are isostructural and crystallize in the triclinic $P\bar{1}$ space group with two donors and one anion per unit cell. Since most electronic density lies symmetrically on both sides of the flat TM molecules, the best optimization to the cohesive energy coming from the delocalized carriers is achieved when the donors stack is in a plane to plane configuration giving rise to an electron delocalization along the stacking

direction. Two organic molecules per unit cell belonging to the same stack are oxidized and contribute one electron to each unit cell.

Since flat TM organic molecules are not strongly interacting objects in the solid state this confers some relevance in the local point of view in the band structure calculation. In the present case, the starting point is the HOMO state (highest occupied molecular orbital) which is constructed from a linear combination of atomic orbitals of the TM molecule (Figure 3). The use of the extended-Hückel method of quantum chemistry then leads to an appropriate description of the band formation in these narrow band systems. Most band structure calculations reported so far, however, have been made using a 2-D model [37, 38, 39], 3D calculations have been performed more recently for $(\text{TMTTF})_2\text{Br}$ and $(\text{TMTSF})_2\text{PF}_6$ [40]. The tight-binding band of all compounds looks like the typical dispersion relation in Fig. 6. The band structure parameters thus obtained can be used to define the following model of the energy spectrum:

$$\epsilon(\mathbf{k}) = -2t_a \cos(k_a a/2) - 2t_{\perp b} \cos(k_{\perp b} b) - 2t_{\perp c} \cos(k_{\perp c} c). \quad (1)$$

where it is assumed that the underlying lattice is orthorhombic. The symmetry of the lattice in the $(\text{TM})_2\text{X}$ being triclinic, the above expression then represents a simplified model of the actual spectrum of Figure 6 but it retains the essential and is easier to manipulate. The conduction band along the chain direction has an overall width $4t_a$ ranging between 0.4 and 1.2 eV, depending on the chemical nature of the donor molecule. As the overlap between the electron clouds of neighboring molecules along the stacking direction is about 10 times larger than the overlap between the stacks in the transverse b direction and 500 times larger than that along the c direction the electronic structure can be viewed at first sight as one-dimensional with an open and slightly warped Fermi surface centered at the Fermi wave vector $\pm k_F^0$ defined for isolated chains (Figure 6).

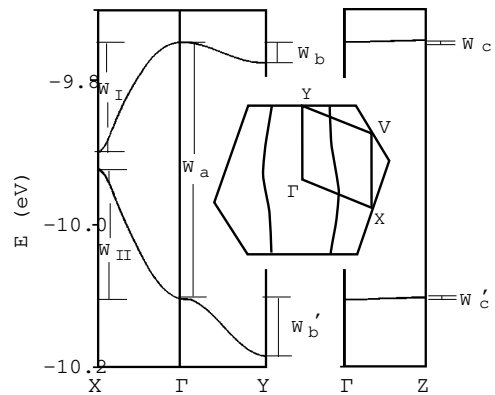


Figure 6: Electronic dispersion relation and projected 2D Fermi surface for $(\text{TMTTF})_2\text{Br}$ calculated on the basis of its room temperature and ambient pressure structure, after [40].

S	(TMTTF) ₂ PF ₆	(TMTTF) ₂ Br	(TMTSF) ₂ PF ₆	(TMTSF) ₂ ClO ₄
d ₁ (Å)	3.52	3.50	3.68	3.63
d ₂ (Å)	3.62	3.53	3.66	3.64
t ₁ (meV)	137	133	252 (39%)	258 (39%)
t ₂ (meV)	93	119	209 (33%)	221 (33%)
W _a (meV)	463	469 (35%)	884 (49%)	878 (12%)
W _b (meV)	55 (52)	37 (30)	130 (70)	96 (14%)
W _c (meV)	49	107	206	256
W _d (meV)	2 ^a			2 ^a
W _e (meV)	2 ^a			2 ^a

Table 1: Intrastack crystallographic data and calculated band parameters for members of the (TM)₂X series, after [39], ^a[40], and ^b[37].

The anions located in centrosymmetrical cavities lie slightly above or below the molecular planes. This structure results in a dimerization of the intermolecular distance (overlap) with a concomitant splitting of the HOMO conduction band into a filled lower band separated from a half-filled upper (hole-like) band by a gap Δ_D at $\pm 2k_F^0$, called the dimerization gap which is shown in Fig. 6 at the point X of the new Brillouin zone. However, on account of the transverse dispersion, this dimerization gap does not lead to a genuine gap in the density of states as shown from the extended-Hückel band calculation (Figure 7). The only claim which can be made is that these conductors have a commensurate band filling (3/4) coming from the 2:1 stoichiometry with a tendency towards half filling which is more pronounced for sulfur than for selenium compounds, while it differs from compound to compound within a given series.

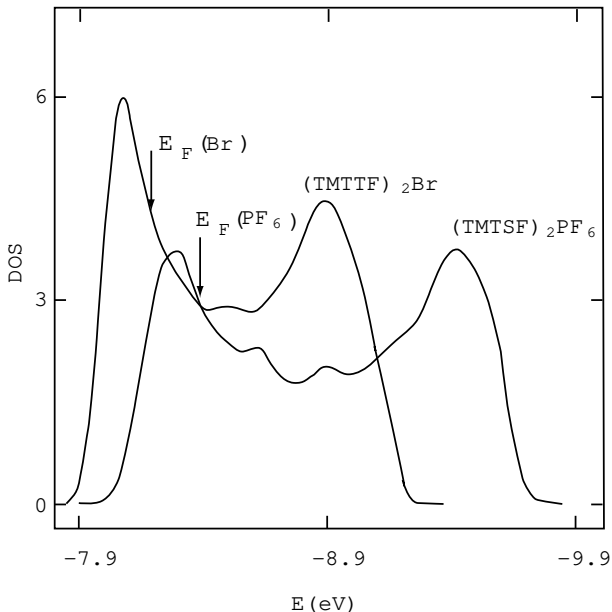


Figure 7: Electronic density of states of (TMTTF)₂Br and (TMTSF)₂PF₆. Courtesy of E. Canadell.

2.1. Role of anions

The possibility for (TM)₂X compounds having non-centrosymmetrical anions to undergo a structural phase transitions can modify the band structure and the topology of the Fermi surface. Anions such as ClO₄, ReO₄, NO₃, SCN etc., have two equivalent orientations corresponding to short and long contacts between Se (resp. S) atoms of TMTSF (resp. TMTTF) molecule and a peripheral electronegative atom of the anion. Consider the case of (TMTSF)₂ClO₄, the anion lattice orders at 24K leading to a superstructure of the Se-O contacts with a wave vector $\mathbf{q}_A=(0, \frac{1}{2}, 0)$ – here expressed in units of the reciprocal lattice vector [41, 42]. The periodic potential thus created connects two Fermi points along the *b* direction and opens a gap which doubles the unit cell along that direction. The folding of the Fermi surface that results introduces two warped Fermi surfaces near $\pm k_F^0$. Anion lattice superstructure has thus important consequences on one-particle spectrum and its symmetry properties – the nesting of the Fermi surface. This plays an important role in the strength of electron-electron interactions at low temperature. It also influences the stability of the superconducting phase in (TMTSF)₂ClO₄ below 1.2 K at ambient pressure and the variety of features induced by a magnetic field such as the so-called quantization of the Fermi surface nesting in the spin-density-wave phase ordering [43, 44, 45, 46], and the Lebed resonances [47]. This is particularly manifest when it is compared to compounds with spherical anions such as PF₆, AsF₆, etc., for which the absence of alteration of the Fermi surface via anion ordering entails for example the stabilization of spin-density-wave long-range order at ambient pressure.

For other compounds with a non-centrosymmetrical anion like ReO₄, the structural ordering is different and takes place at $\mathbf{q}_A=(\frac{1}{2}, \frac{1}{2}, \frac{1}{2})$; its impact on the electronic structure, however, turns out to be more marked since the anion potential at this wave vector creates a gap over the whole Fermi surface which is so large in amplitude ($\sim t_a$) that it leads to an insulating state in which electron-electron interactions probably play little role. The application of hydrostatic pressure is then required to restore the metallic state and the possibility of long-range ordering for electronic degrees of freedom [48].

As previously mentioned, the anion potential produced by spherical anions like PF₆, AsF₆,..., leads to a modulation of the charge along the organic stack with the same periodicity as the dimerization [49]. It may independently contribute to the half-filled character of the band and then enhances the strength of electron-electron interaction at low temperature [50].

3. Normal state: Fermi liquid description

Although the relevance of electron-electron interactions is in general not disputed in (TM)₂X, it is on the point of their magnitude and their magnification – as a consequence of low-dimensionality in a experimentally accessible part the normal phase – that opinions differ. Let us consider the point of view where the interacting fermions of the normal phase are described within the Fermi liquid picture. By doing so in the present case, all the complications of one-dimensional physics and the concomitant correlation and

Luttinger liquid effects turn out to be relegated at high-energy or temperature.

A rough, zero-order, estimate of the extent to which a Fermi liquid description would be viable in the normal phase is provided by the scale of $t_{\perp b}$ given by band calculations. Consider the temperature range $T \ll t_{\perp b}$ ($k_B = 1$), where thermal fluctuations are sufficiently weak to lower the uncertainty on the transverse band wave vector to a range of values $\delta k_{\perp b} \ll 1/d_{\perp b}$, that is small compared to the size of Brillouin zone. The band wave vector $k_{\perp b}$ is therefore a good quantum number so the transverse band motion and the curvature of the Fermi surface are coherent. Otherwise, when $T > t_{\perp b}$, one has $\delta k_{\perp b} > d_{\perp b}^{-1}$, which is large enough for the curvature of the Fermi surface to be blurred by thermal effects; quantum coherence of electrons is then perpendicularly disrupted and is thermally confined to small distance $\delta r_{\perp b} < d_{\perp b}$ (which actually coincides with the perpendicular de Broglie wavelength), thereby making the relevant physics essentially one-dimensional in character. In this simple description the characteristic temperature scale $T_{x1} \sim t_{\perp b}$ then signals a gradual change of dimensionality or a crossover in the properties at the one-particle level [50].

According to band calculations (see Table 1), $t_{\perp b}$ is around 200K in systems like (TMTSF)₂X, while it is slightly less in (TMTTF)₂X. This figure being large compared to the corresponding scale for long range order ($\sim 1\text{K} \dots 20\text{K}$), most part of the normal state below room temperature should then be correctly described by a Fermi liquid picture. In this scenario, the quasi-particle motion, albeit anisotropic, is influenced by the interactions with other particles through some kind of a mean-field effect. The energy spectrum thus keeps the same form as (1), except for a renormalization of the effective mass of the quasi-particle in each direction. One can then write for the spectrum

$$\epsilon_p^*(\mathbf{k}) - \mu = v_F^*(pk - k_F^0) - \sum_{i=b,c} 2t_{\perp i}^* \cos(k_{\perp i} d_{\perp i}), \quad (2)$$

where in the spirit of the Fermi liquid theory, the longitudinal part of the spectrum has been linearized around the 1D Fermi points $pk_F^0 = \pm\pi/2a$, $v_F^* = k_F^0/m^*$ ($\hbar = 1$) is the effective Fermi velocity and m^* the effective mass along the chain direction. As for the transverse part, we have kept the tight-binding structure of the spectrum which is assumed to be unaltered by the physics taking place at high energy. This form is essential in order to preserve the symmetry properties of the spectrum and an open Fermi surface. Here $t_{\perp b,c}^*$ denote the effective – renormalized – transfer integrals along b and c directions. This renormalization, which actually results from the ‘history’ of the system at high energy – where it is presumably 1D – will in turn affect the crossover temperature that is, $T_{x1} \sim t_{\perp b}^*$ [51].

3.1. Fermi liquid properties at equilibrium

Susceptibility. – In the Fermi liquid picture, static and uniform response function like the spin susceptibility χ_s is also renormalized with respect to the ideal Fermi gas prediction. It takes the form [52]

$$\chi_s = \frac{2\mu_B^2 N(E_F^*)}{1 + F^a}, \quad (3)$$

where μ_B is the Bohr magneton and $N(E_F^*) = (\pi v_F^*)^{-1}$ is the electronic density of states per spin. Here F^a is an effective coupling constant which favors spin alignment and then leads to an enhancement of the susceptibility for repulsive interaction ($F^a < 0$). Although this constant is phenomenological in the framework of the Fermi liquid theory, a straightforward connection between F^a and a microscopic model like the Hubbard model can be made through a first-order Hartree-Fock calculation – which is actually equivalent to a static Random Phase Approximation (RPA). One then finds $F^a = -N(E_F) aU$, where U is the short-range Coulomb repulsion parameter of the Hubbard model. Thus in the Hartree-Fock picture, the amplitude of $U/4t_a$ for different compounds can be extracted from the ratio χ_s/χ_s^0 between the observed susceptibility in the very low temperature region [53, 54] and its calculated value using the band parameters extracted from experiments or from band calculations [55]. For systems like (TMTSF)₂ClO₄ (respectively (TMTTF)₂PF₆), one finds $\chi_s/\chi_s^0 \simeq 2$ (respectively, $\chi_s/\chi_s^0 \simeq 3$), which leads to $U/4t_a \simeq 0.3$ (respectively, $U/4t_a \simeq 0.4$) for a quarter-filled band. This simple analysis of the spin susceptibility thus indicates the presence of moderate Coulomb repulsion. They are however less than the values determined from elaborate quantum chemistry calculations made for U at the molecular or local level [56, 57], which lead to $U/4t_a \simeq 4 - 8$. The difference may be attributed to the fact that at variance with quantum chemistry method, the Fermi liquid theory is a low-energy theory and the interaction parameter F^a reflects a screened rather than a local quantity.

The Fermi liquid as well as the Hartree-Fock theory, however, can hardly account for the observed temperature dependence of the spin susceptibility obtained at constant volume – namely, corrected for thermal dilatation of the sample – which shows a monotonic but sizable growth as the temperature increases (Figure 8) [53, 54, 58]. This variation turns out to be much faster than the one expected from the H-F theory, which only predicts a $F^a(T)$ with a very slow temperature dependence that is spread out over E_F on a temperature scale [58, 59].

Specific heat. – In the Fermi liquid theory, the expression for the electronic contribution to the specific heat is linear in temperature $C_e(T) = \gamma T$, where the Sommerfeld constant is

$$\gamma = \frac{2}{3}\pi^2 N(E_F^*). \quad (4)$$

The strength of interaction can also be provided through the Wilson ratio [60]

$$R_W = \frac{\pi^2}{3\mu_B^2} \frac{\chi_s}{\gamma} = \frac{1}{1 + F^a}. \quad (5)$$

Deviations of R_W from unity thus give information about the amplitude of interactions.

The first measurements of the temperature dependent specific heat in the normal state of the Bechgaard salts were made by Garoche *et al.* on (TMTSF)₂ClO₄ [61]. After subtraction of the phonon contribution, the electronic part of the specific heat, albeit restricted to the very low temperature domain shows the metallic linear behavior $C_e = \gamma T$ (Figure 9). The evaluation of the Sommerfeld constant

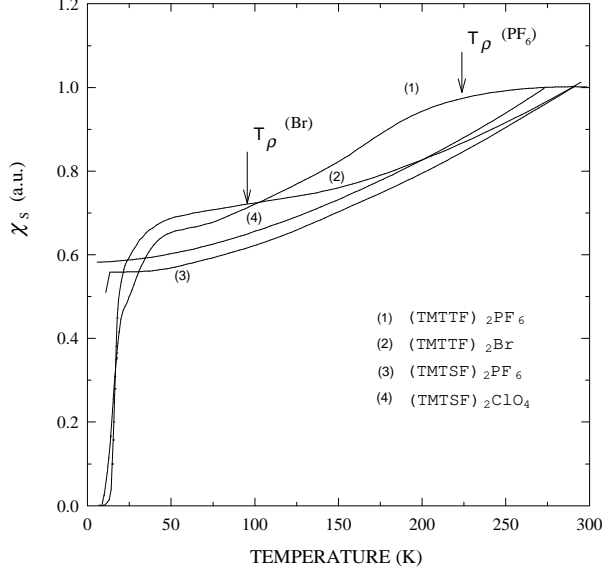


Figure 8: Temperature dependence of the magnetic spin susceptibility of members of (TM)₂X series. The arrows indicate the temperature scale T_ρ for the onset of the insulating behavior in the resistivity for (TMTTF)₂PF₆ and (TMTTF)₂Br (see Fig. 4).

$\gamma \simeq 10 \text{ mJ} \cdot \text{mole}^{-1} \cdot \text{K}^{-2}$ allows a determination of the density of states $N(E_F^*) \simeq 1 \text{ states/eV/spin/molecule}$, in fair agreement with the one obtained from the low temperature value of the spin susceptibility according to the analysis of Miljak *et al.* [53], thereby lending support to a weak coupling Fermi liquid picture in this temperature domain. The analysis of Miljak *et al.*, of the spin susceptibility and the electronic specific heat of (TMTSF)₂ClO₄ then suggests that F^a is not large in this system, at least in the low temperature range.

On the other hand, the electronic specific heat reveals an important field dependence [62] (Figure 10). The linear specific heat coefficient γ increases from $10 \text{ mJ} \cdot \text{mol}^{-1} \cdot \text{K}^{-2}$ at low field (although larger than the critical field $H_{c2} = 1 \text{ kOe}$ along c^*), and passes through a maximum of $25 \text{ mJ} \cdot \text{mol}^{-1} \cdot \text{K}^{-2}$ at $H_m = 20 \text{ kOe}$ for $T \approx 1 \text{ K}$. The locus of the points corresponding to the maximum of γ in the $H - T$ plane is located in the paramagnetic domain of (TMTSF)₂ClO₄, i.e. not to be confused with the onset of a field-induced spin-density-wave state detected by the same specific heat technique [63]. Hence, the observed decrease of the Wilson ratio R_W under magnetic field is a peculiar property of this low temperature electron gas which hardly fits with the Fermi liquid model. Furthermore this experimental finding is reminiscent of the expected behavior in a slightly doped Mott insulator as the metal-insulator transition is approached (i.e. band filling approaching half-filling). Anomalous magnetoresistance is also seen for similar and larger field in a broad range of temperature in the normal phase [32].

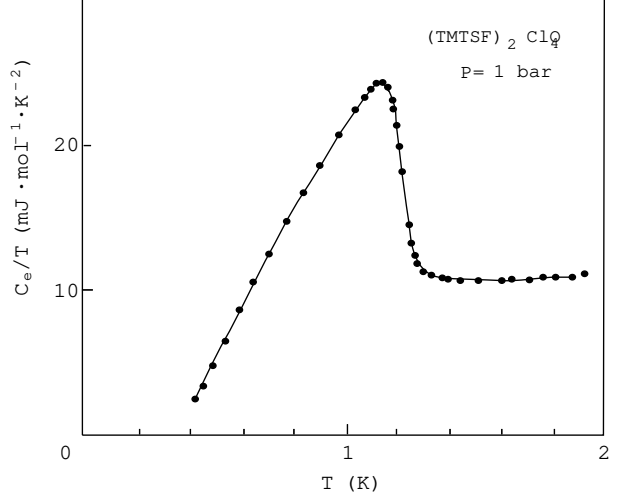


Figure 9: Specific heat as a function of temperature in (TMTSF)₂ClO₄ near the superconducting transition, after ref. [61].

3.2. Fermi liquid close to equilibrium: dynamics

Key features of both the non-interacting and the interacting Fermi liquid theory can be illustrated through the retarded one-particle Green function, which can be defined from the following Fourier transform

$$G_p(\mathbf{k}, \omega) = -i \int e^{i\omega t} \langle \text{GS} | T_t a_{p,\mathbf{k},\sigma}(0) a_{p,\mathbf{k},\sigma}^\dagger(t) | \text{GS} \rangle dt$$

taken in the ground state. In a non-interacting Fermi gas, it takes the form

$$G_p(\mathbf{k}, \omega) = \frac{1}{\omega - \epsilon_p(\mathbf{k}) - i \text{sgn}(\epsilon_p) 0^+}, \quad (6)$$

where we have redefined $\epsilon_p(\mathbf{k}) - \mu \rightarrow \epsilon_p(\mathbf{k})$. The singularities in the imaginary part $\text{Im}G_p(\mathbf{k}, \omega) = \pi \delta(\omega - \epsilon_p(\mathbf{k}))$ indicates that the particle and the hole states are the true eigenstates of the system. As the interaction is turned on there is a one-to-one correspondence between these non-interacting states and the quasi-particle states of the interacting Fermi liquid. This is possible close to the Fermi surface where the decay rate of quasi-particles is sufficiently slow compared to the branching time of interaction. Consequent to this correspondence, the quasi-particles states are labeled by the same quantum numbers (\mathbf{k}, σ) and the coherent part of the one-particle Green function for a Fermi liquid takes the form

$$G_p(\mathbf{k}, \omega) = \frac{z}{\omega - \epsilon_p^*(\mathbf{k}) - i \text{sgn}(\epsilon_p^*) \tau_{\mathbf{k}}^{-1}}, \quad (7)$$

where z is the quasi-particle weight which actually corresponds to the amplitude of the step of the quasi-particle distribution function $n[\epsilon_p^*(\mathbf{k})]$ in a Fermi liquid ($z = 1$ in a non-interacting Fermi gas). Inelastic collisions introduce incoherent scattering and an imaginary part in the quasi-particle energy, which is translated into a decay rate of quasi-particles [64, 29, 34],

$$\tau_{\mathbf{k}}^{-1} \sim g_3^2 \max[\omega^2, T^2, (\epsilon_p^*(\mathbf{k}))^2] \quad (8)$$

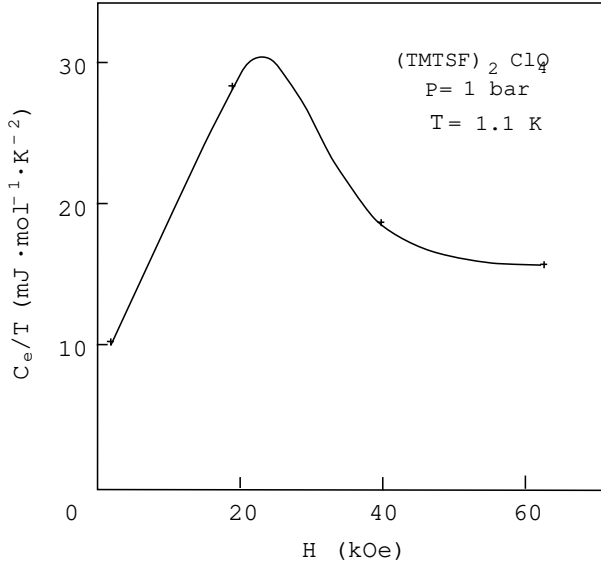


Figure 10: Magnetic field dependence of the Sommerfeld constant of specific heat in $(\text{TMTSF})_2\text{ClO}_4$ at low temperature.

where g_3 is an electron-electron coupling constant that does not conserve momentum (Umklapp scattering). The lifetime of quasi-particles becomes infinite at \mathbf{k}_F ($\tau_{\mathbf{k}_F}^{-1} = 0$) due to the exclusion principle which severely restricts the possibility of scattering events as we approach the Fermi surface. Thus at \mathbf{k}_F , the delta function singularity in the imaginary part $\text{Im}G_p(\mathbf{k}, \omega) = \pi z \delta(\omega - \epsilon_p(\mathbf{k}))$ indicates that at the Fermi level quasi-particles become eigenstates.

Other features of a Fermi liquid emerge when a perturbation that is slowly varying in space and time is coupled either to spin or charge degrees of freedom. The mean-field that wraps up each quasi-particle in a Fermi liquid acts as a coherent restoring force that leads to a collective response of the system as a whole. One then finds two types of collective or sound modes, namely the charge (or the plasmons for a metal) and the spin (paramagnons) modes [52].

Consider for example the paramagnons of an anisotropic 2D Fermi liquid as described by the one-electron spectrum (2) with $t_{\perp c}^* = 0$; the imaginary part of the retarded spin response function at low frequency is found to be

$$\text{Im}\chi(\mathbf{q}, \omega) = \chi_s \frac{\omega_\sigma(\mathbf{q})\omega}{\omega_\sigma^2(\mathbf{q}) + \omega^2}. \quad (9)$$

The absence of pole on the real axis in this expression indicates – as it is the case for isotropic Fermi liquid [52] – strong damping of paramagnons. Nonetheless, the spectral weight shows a peak at

$$\omega_\sigma(\mathbf{q}) = 2(1 + F^a) \sqrt{(v_\perp^* q_\perp)^2 - (v_F^* q)^2}, \quad (10)$$

which stands as the dispersion relation of paramagnons where $v_\perp^* = 2t_{\perp b}^*/b$. As a result of the peculiar anisotropic form of the electronic spectrum (2), the available phase space for 2D paramagnons is reduced so spin excitations are only defined for $v_\perp^* q_\perp > v_F^* q$.

NMR nuclear spin relaxation. – The temperature and the magnetic field variation of the nuclear spin-lattice relaxation (T_1^{-1}) as obtained by Nuclear Magnetic Resonance is known to be a quite useful tool for the characterization of spin dynamics in metals [65, 66]. Given the local coupling between a NMR-active nuclear spin and the electronic spin density through the hyperfine coupling, the study of the relaxation process of the nuclear spin gives useful information about the statics, the dynamics and the effective dimensionality D of electronic spin correlations of different wave vectors q [67, 68]. This opportunity given by the T_1^{-1} measurements has been recognized from the start in the study of the ordered and normal states in the Bechgaard salts and their sulfur analogs. The analysis of the nuclear relaxation essentially focus on the following basic expression due to Moriya [65] :

$$T_1^{-1} = 2\gamma_N^2 |A|^2 T \int d^D q \frac{\text{Im}\chi(\mathbf{q}, \omega)}{\omega}, \quad (11)$$

where γ_N is gyromagnetic ratio of the nucleus, A is proportional to the hyperfine matrix element, and $\text{Im}\chi(\mathbf{q}, \omega)$ is the imaginary part of the dynamic spin susceptibility at wave vector \mathbf{q} and Larmor frequency ω . As we have seen, spin fluctuations of an interacting Fermi liquid consist exclusively of long wavelength damped paramagnons which according to (9), are considered as non-diffusive and for which one finds:

$$T_1^{-1}[\mathbf{q} \sim 0] = CT\chi_s^2, \quad (12)$$

Thus for a 2D Fermi liquid, the enhancement of the nuclear relaxation with respect to the non-interacting ‘Korringa limit’ $T_1^{-1} \propto T[N(E_F)]^2$, grows as the square of the enhancement of the susceptibility¹.

The experimental situation in $(\text{TMTSF})_2\text{X}$ and $(\text{TMTTF})_2\text{X}$ salts does reveal an enhancement of the relaxation rate with respect to the Korringa law which is compatible with the above expression at high enough temperature (Figure 11). Detailed investigations of χ_s and T_1^{-1} data for several members of both $(\text{TMTTF})_2\text{X}$ and $(\text{TMTSF})_2\text{X}$ series show that the relation $T_1^{-1} \propto T[\chi_s(T)]^2$ is apparently well satisfied over a large temperature domain of the normal phase. Although this could support the Fermi liquid theory in this sector of the normal phase, it has been shown, however, that 1D – undamped – paramagnons of a Luttinger liquid leads to a similar expression for T_1^{-1} near $q = 0$ [67]. Moreover, following the example of the temperature dependence of susceptibility, the FL prediction fails to account for the temperature dependence of the enhancement, which according to Figure 11, shows a too large variation [58, 67].

The Fermi liquid theory is more seriously flawed in the low temperature part of the normal phase where pronounced deviations to (12) have been reported for all compounds studied in $(\text{TMTTF})_2\text{X}$ and $(\text{TMTSF})_2\text{X}$ series. In this temperature range, the variation of $(T_1 T)^{-1}$ shows an important increase instead of the expected decrease and its

¹It should be noted here that the expression for the relaxation rate slightly differs when paramagnons induce weak ferromagnetism. In this case, $(T_1 T)^{-1} \sim [\chi_s]^{\frac{1}{2}(5-D)}$ varies as a power of the spin susceptibility whose index depends on the spatial dimensionality D [67].

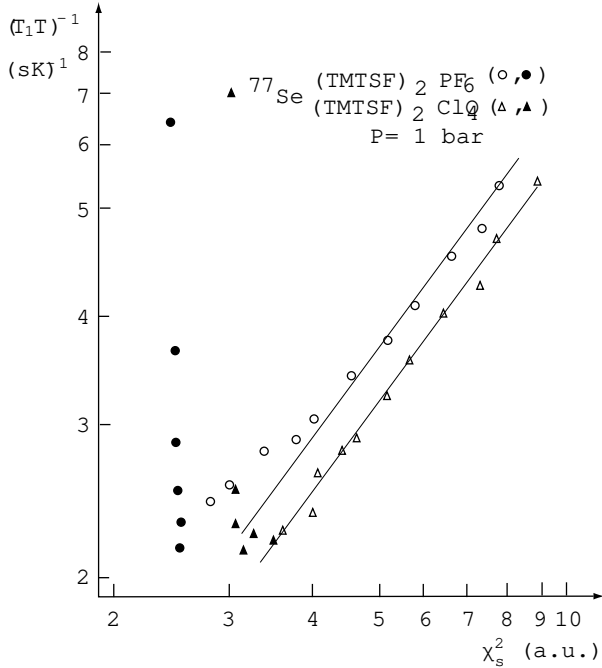


Figure 11: ^{77}Se enhancement $(T_1T)^{-1}$ as a function of the square of the measured susceptibility for $(\text{TMTSF})_2\text{PF}_6$ and $(\text{TMTSF})_2\text{ClO}_4$, after ref. [67].

occurs in a temperature region where the magnetic susceptibility does not show any appreciable variation. This enhancement was first reported in the case of $(\text{TMTSF})_2\text{ClO}_4$ (Figure 12) [51, 69, 70]; it was afterwards invariably found in all members of the $(\text{TMTSF})_2\text{X}$ and $(\text{TMTTF})_2\text{X}$ series with more or less the same profile in temperature depending on the nature of the ground state. In a compound like $(\text{TMTSF})_2\text{PF}_6$ at ambient pressure, the anomalous contribution to the enhancement is found to grow by a factor around five between 200 K and 50 K that is, well outside the critical domain associated to the spin-density-wave transition at $T_N \simeq 12$ K [67, 58]; it is even stronger for members of the $(\text{TMTTF})_2\text{X}$ series where a singular enhancement of the form $(T_1T)^{-1} \sim T^{-1}$ (or $T_1^{-1} \sim \text{constant}$) is invariably found (see Figure 25) [58]. Emerging very deeply in the normal phase, this anomalous behavior of nuclear relaxation has played an important part of the debate surrounding the limitations of the FL theory to describe the normal phase of these quasi-one-dimensional conductors. Following the first observations made on $(\text{TMTSF})_2\text{ClO}_4$, it was propounded that this additional contribution to the relaxation rate originates in antiferromagnetic spin fluctuations which are essentially one-dimensional in character (Figure 12).

As the temperature is increased in the normal state the electron lifetime decreases according to (8), it follows that the dynamics of paramagnons gradually moves away from the collisionless to the diffusive limit when $\omega_e\tau \ll 1$, where ω_e is the electronic Larmor frequency. Probing diffusive spin dynamics is possible through the field dependence of the nuclear spin-lattice relaxation rate; being sensitive to dimensionality of the spin system it can give – whenever it is present – quite useful information about the effective

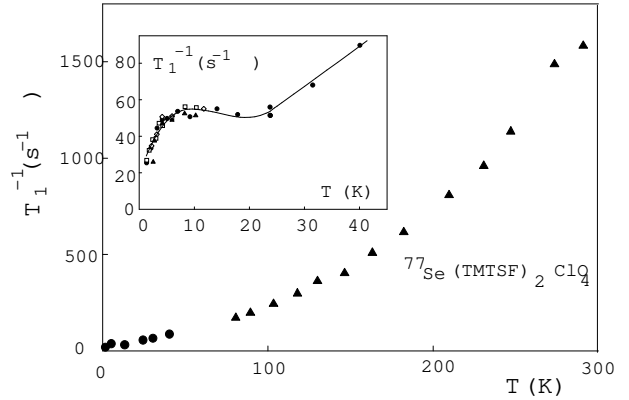


Figure 12: ^{77}Se T_1^{-1} vs T data of $(\text{TMTSF})_2\text{ClO}_4$, after [58, 51].

dimensionality of spin dynamics in organic conductors [66, 71, 72, 73]. Focusing on the field dependence of the paramagnon contribution as a function of the spatial dimensionality D , one finds

$$\begin{aligned} T_1^{-1} &\sim (\omega_e\tau)^{-\frac{1}{2}} \quad (D = 1), \\ T_1^{-1} &\sim \ln \frac{1}{\omega_e\tau} \quad (D = 2), \\ T_1^{-1} &\sim \text{constant} \quad (D = 3). \end{aligned} \quad (13)$$

The search for a field dependence of the nuclear relaxation rate in the normal phase of $(\text{TMTSF})_2\text{ClO}_4$ has been set out by Caretta *et al.* [74]. Their results obtained at 200 K (Figure 13) up to 15 Tesla show a square-root field dependence which is indicative of one-dimensional diffusive spin dynamics. The square root dependence is cut off at low enough field due to processes that do not conserve spin along the stacks [66]. The field dependence is found to become essentially undetectable around 150 K and below, which may indicate either a change of dimensionality in the spin dynamics or that the collisionless regime is reached.

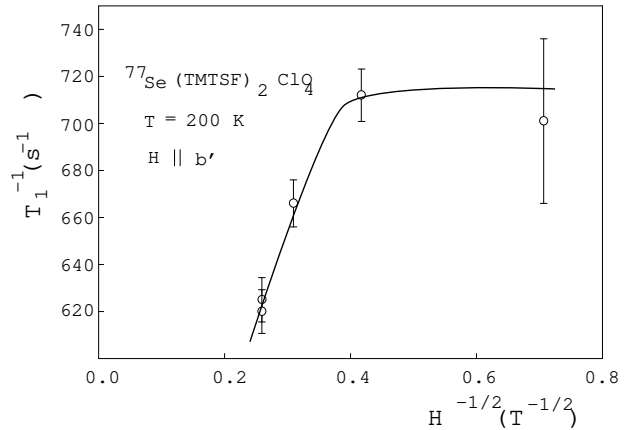


Figure 13: Field dependence of the ^{77}Se nuclear spin-lattice relaxation rate in $(\text{TMTSF})_2\text{ClO}_4$, after [74].

Earlier investigations of Azevedo *et al.* [73], obtained on ^1H of $(\text{TMTSF})_2\text{PF}_6$ in the high-pressure metallic phase

at very low temperature revealed the existence of a field dependence of T_1^{-1} at 4 K up to a field of 10 kOe, which has been held to fit in with the logarithmic profile expected for diffusive two-dimensional spin dynamics (Eq. 13).

Transport: (TMTSF)₂X. – In a metallic system where phonons and impurities play little role in the scattering rate of carriers, the temperature dependence of resistivity is controlled by electron-electron scattering rate. In a Fermi liquid, it is then governed by the decay rate of quasi-particles. Dropping the logarithmic factors due to either the special geometry of the Fermi surface or the proximity of the SDW transition, one gets a quadratic temperature dependence of the form [29, 75, 34]:

$$\rho(T) \propto \tau_{\mathbf{k}_F}^{-1} \sim T^2. \quad (14)$$

Within the Fermi liquid picture this temperature dependence for the resistivity should hold for at least two spatial directions at $T \ll T_x$.

Before making any comparison with actual data in systems like (TMTSF)₂X, one should be aware of the remarkably strong pressure (or volume) dependence of the transport properties. The longitudinal conduction of (TMTSF)₂X increases at a rate of $\approx 25\%$ kbar⁻¹. This pressure coefficient is significantly larger than the figure expected for a scattering mechanism governed by acoustic phonons in the Boltzmann formalism since the pressure dependence of the bare bandwidth is of order 2% kbar⁻¹ in 1-D organic conductors as measured either from the pressure dependence of the longitudinal plasma edge [76], or from the pressure dependence of the Fermi wave vector in TTF-TCNQ [77].

Owing to the significant pressure dependence of $\rho_a(T)$ observed down to low temperature, the temperature variation of the resistivity measured under constant pressure contains two contributions. One is coming from the temperature dependence of the scattering processes and another one is related to the volume dependence of these processes through the thermal contraction of the lattice. In order to obtain experimental data which can be confronted to the theory the observed temperature dependence under constant pressure must be transformed into a constant volume dependence. As some arbitrariness remains in the conversion procedure, the converted data must be considered at best as an improvement before comparison with the theory is made. The unit cell of the crystal at 50 K has been taken as the reference unit cell (such an hypothesis being justified by the lack of thermal expansion at this temperature). The procedure goes as follows. At a temperature T above 50 K, a pressure P is needed in order to recover the reference volume. An important simplification of the procedure has been made assuming that the cell length along a is the most relevant parameter (instead of the volume) to be taken into account. Hence, thermal expansion, compressibility data and isobaric temperature dependence of the resistivity enable a point by point derivation of the temperature dependence at constant volume which is displayed in Fig. 14.

This conversion procedure must be attempted for the longitudinal as well as for the transverse transport. The results for $\rho_a(T)$ in (TMTSF)₂PF₆ at ambient pressure is given in Fig. 14 where a crossover from a superlinear to a

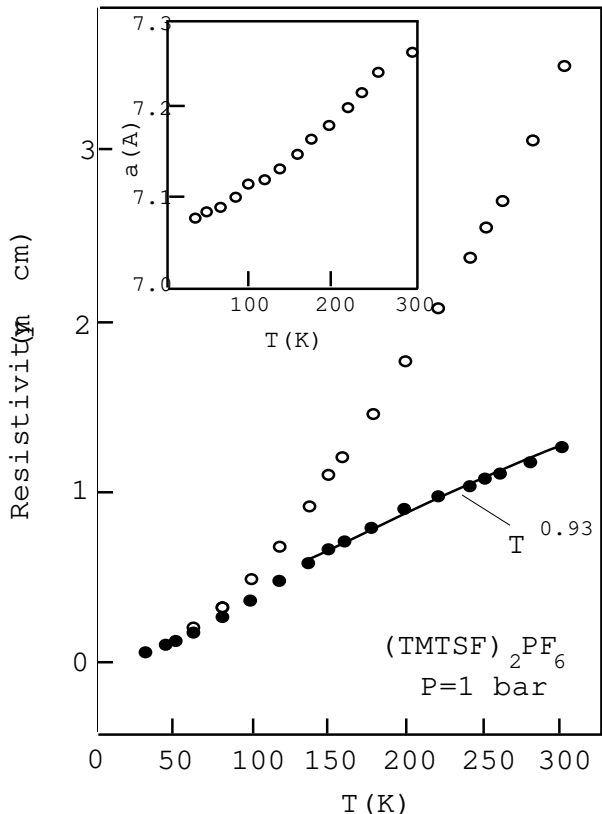


Figure 14: Longitudinal resistivity of (TMTSF)₂PF₆ as a function of temperature at constant pressure (open circles, Ref. [78]) and converted to constant volume (full circles). In the inset, the variation of the stack lattice parameter with temperature after [79].

linear (or sublinear) power law temperature dependence is observed in the vicinity of 80 K. A detailed analysis based on the Fermi liquid theory shows that a T^2 law is apparently well satisfied below 50 K down to the vicinity of the spin-density-wave transition where the resistivity is dominated by critical scattering effects [75].

The resistivity measurements along the transverse c direction are also interesting. Actually one can infer that σ_c is directly related to the physics of the $a-b$ planes and therefore could probe whether transport proceeds via collective modes or independent quasi-particles. Jacobsen *et al.* [80], were the first to report a non-monotonic temperature dependence of ρ_c in (TMTSF)₂PF₆ passing through a well characterized maximum at $T_m = 80$ K (under ambient pressure) ‘at variance’ with the T -dependence in the a direction [80]. A recent pressure study of this effect has shown that T_m evolves under pressure and reaches about 300 K at 10 kbar [81]. The constant volume data for $\rho_c(T)$ in the ‘metallic’ regime below T_m reveals that $\rho_c(T) \propto T^{1.5}$, which differs from a T^2 law and may indicate that the transport along the less conducting axis is incoherent and diffusive since this temperature region is still characterized by $T \gg t_{1c}^*$. As for DC resistivity measurements along b they are more difficult to be neatly realized owing to non-uniform current distributions between contacts which introduce

contributions coming from other directions. Nevertheless, if we apply a tunneling argument between the $a - b$ planes instead of chains that is, if quasiparticle states with mean free paths of order $\tau_a t_a / \hbar$ and $\tau_b t_{\perp b} / \hbar$ can be defined along a and b directions respectively, the transverse conductivity reads $\sigma_c \approx (\sigma_a \sigma_b)^{1/2}$ [81]. Hence, provided the quasi-particle life times along a and b exhibit the same temperature dependencies the anisotropy ratio ρ_c / ρ_a should be T -independent. This is definitely not observed below T_m as experimental laws such as $\rho_a(T) \approx T^2$ and $\rho_c(T) \approx T^{1.5}$ are more appropriate leading to $\rho_b(T) \approx T$ within the quasi-particle hypothesis for the $a - b$ planes. A linear temperature dependence is indeed very close to the early experimental findings for $\rho_b(T)$ below T_m under ambient pressure suggesting that the quasi-particle states if they can be defined at all are not Fermi-liquid-like but possibly marginal.

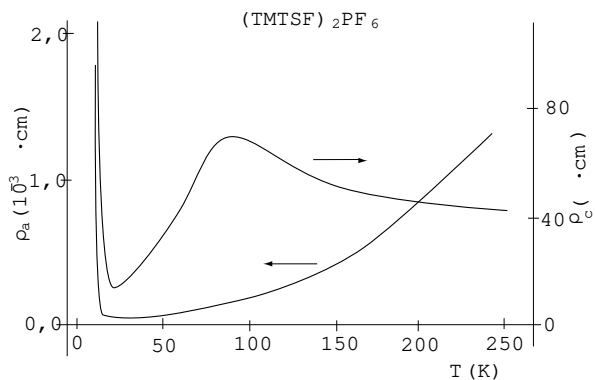


Figure 15: Longitudinal and transverse c resistivities as a function of temperature in $(\text{TMTSF})_2\text{PF}_6$, after [81].

Very recently, Fertey *et al.* [82], showed that a direct measurement of $\rho_b(T)$ on a system like $(\text{TMTSF})_2\text{PF}_6$ is possible using the microwave technique and the results show the existence of a maximum of $\rho_b(T)$ as a function of temperature around 40 K – which is somewhat lower than the value of T_m shown by $\rho_c(T)$.

The striking different temperature dependencies for the *in* and *out* of plane resistances suggest an interpretation in terms of a non-Fermi liquid approach for $T > T_m$, although $\rho_a(T)$ is not far from a conventional behavior. The Figure 15 emphasizes the remarkable feature of $(\text{TMTSF})_2\text{PF}_6$, namely, opposite temperature dependencies for interplane and chain resistivities above T_m . A temperature independent anisotropy ratio is indeed observed below 10 K in $(\text{TMTSF})_2\text{PF}_6$ under 9 kbar, suggesting a recovery of the usual Fermi liquid behavior (Figure 16).

Transport: (TMTTF)2X.– Deviations to the Fermi liquid behavior are particularly revealing for $(\text{TMTTF})_2\text{X}$ compounds for which there is a loss of the metallic character at a characteristic temperature T_ρ that can be in magnitude far above the critical temperature domain under low pressure conditions (Figure 4). The scale T_ρ signals a thermal activation of carriers corresponding to a gap $\Delta_\rho \sim 2T_\rho$ in the electrical resistivity of the normal phase. The recent data give $2\Delta_\rho \approx 900\text{K}$ under ambient pressure [81, 84], which

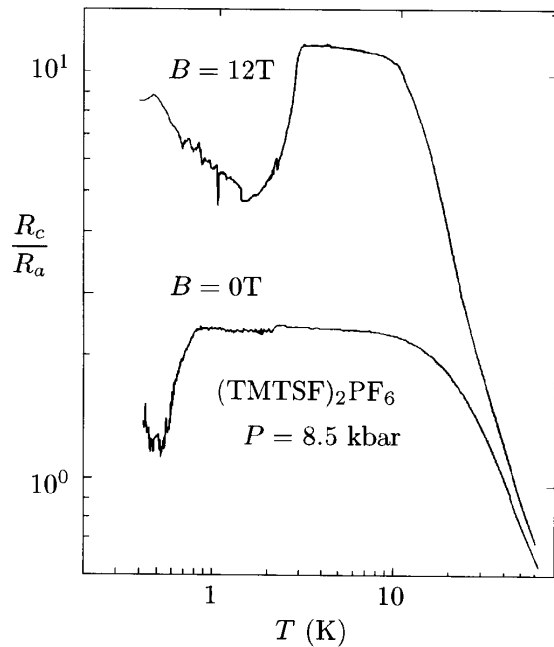


Figure 16: Anisotropy ratio for the resistance along the a and c directions in $(\text{TMTSF})_2\text{PF}_6$, after [83].

only slightly differs from previous estimations [85].

The comparison with the temperature profile of the spin susceptibility is rather striking since the spin susceptibility remains unaffected despite the thermal activation of carriers below T_ρ (see Figures 4 and 8). This apparent decoupling between spin and charge degrees of freedom is in severe contradiction with what should be expected in a Fermi liquid.

Optical properties.– Optical reflectivity measurements performed by Jacobsen *et al.* [86, 87, 88], were probably the first to provide some direct information about the anisotropy of the electronic structure in the Bechgaard salts (Figure 17). The observation of the growth of an infrared reflectance edge in the transverse b' direction of $(\text{TMTSF})_2\text{PF}_6$ below 100 K revealed the presence of a sizable overlap integrals in that direction. Thus the sharpness of a Drude like plasma edge in the b' direction lends support for the gradual emergence of a coherent transverse one-particle motion and a 2D Fermi liquid component in the $a - b$ plane in the temperature region below 100 K. Similar results were subsequently found for other members of the $(\text{TMTSF})_2\text{X}$ series and the analysis of the reflectivity data using a tight-binding spectrum (1) yields $t_{\perp b} \simeq 18 - 22$ meV and $t_{\perp b} / t_a \simeq .1$ for the highest transverse hopping integral and the anisotropy ratio [89, 90]. These values were found to be in a reasonable agreement with the band structure calculations. This would also indicate a small renormalization of $t_{\perp b}$, namely $t_{\perp b}^* \rightarrow t_{\perp b}$ in the energy range of the plasma edge. However it is worth noting that the transverse plasma edge could be insensitive to the quasi-particle renormaliza-

tion factor z in which case, it would only reflect the bare unrenormalized band parameters.

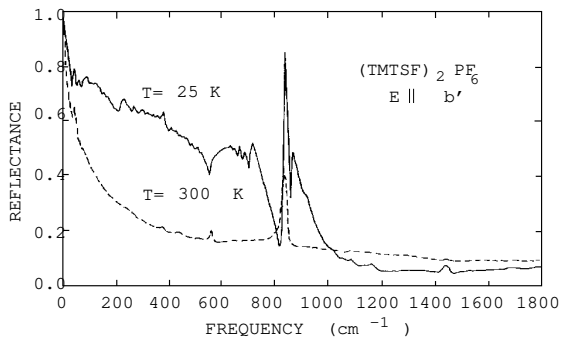


Figure 17: Polarized reflectance for $\mathbf{E} \parallel b'$ of $(\text{TMTSF})_2\text{PF}_6$ at $T = 25\text{K}$ and 300K , after [88].

In contrast, no plasma edge is found along the b and c directions in $(\text{TMTTF})_2\text{X}$ due to the presence of an insulating state. In this case the charge motion perpendicular to the chains is apparently absent and the presence of a charge gap makes the single particle hopping t_{\perp}^* irrelevant at low temperature [91, 92, 93].

The frequency dependence of optical conductivity obtained by Kramers-Kronig transforms of the reflectance data, however, can hardly bow to an analysis based on the Drude model [94, 95]. Despite the large value of DC conductivity in $(\text{TMTSF})_2\text{X}$ materials at low temperature, the amplitude of $\sigma(\omega)$ in the far infrared is much smaller than expected within a simple Drude picture (Figure 18). The absence of a classical Drude peak in the Bechgaard salts was actually reminiscent to what was previously observed in the case of incommensurate CDW system TTF-TCNQ. It was proposed that the narrow zero-frequency peak in conductivity is the result of a collective mode effect that bears some similarity with the sliding a charge-density-wave – especially if one considers the new phonon features that emerge at low temperature [94]. This is all the more surprising if one considers that $(\text{TMTSF})_2\text{X}$ compounds are very good metals in their normal state and that the ground state of these materials is either antiferromagnetic or superconducting. Further, the zero frequency mode is also accompanied by a gap ranging from 160 cm^{-1} to 200 cm^{-1} depending on the compounds. This anomalous feature has been reported by several groups [86, 94, 95, 93]. It was recently proposed to be associated to the remnant of a Luttinger liquid with a correlation gap which is present in the less metallic sulfur series (see the section on the Luttinger liquid)[93, 96].

A different, albeit one-dimensional, interpretation due to Favand and Mila [97], is based on the fact that the energy associated to the dimerization gap falls in the same range of the infrared spectrum. Combined to strong local repulsion among carriers which spreads the single occupancy of the electron states to the band edge, this would lead to a relatively pronounced absorption due to interband transitions [98]. In this scenario, the infrared absorption conductivity shifts to lower frequency when the dimerization

gap decreases as one moves to the right in the phase diagram (Figure 5).

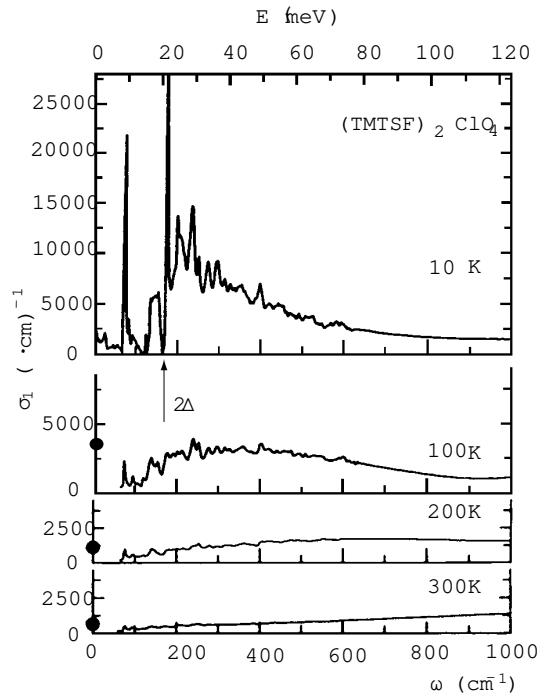


Figure 18: Real part of $\sigma(\omega)$ of $(\text{TMTSF})_2\text{ClO}_4$ along the chain axis at different temperatures in the normal phase. The full circles on the left are the values of DC conductivity. At 10K , there is a gap with the value $2\Delta \simeq 170\text{ cm}^{-1}$. After [94].

A very strong support in favor of an insulating state in $(\text{TMTTF})_2\text{X}$ can also be given by the optical data [88]. The reflectivity spectra reveals the existence of a Drude edge for the light polarized along the a -direction leading to $\omega_p = 8860\text{ cm}^{-1}$ [88]. A Drude model fit based on the band structure (1) or (2) relates the plasma frequency to the band width and leads to either $W_a = 280\text{ meV}$ or 800 meV depending if a $1/2$ -filled or $1/4$ -filled band interpretation is adopted. The former assumption is in fairly good agreement with the ab-initio calculation for $(\text{TMTTF})_2\text{PF}_6$ (see Table I). The optical investigation has been extended recently towards the FIR range showing a leveling-off of the reflectivity at 80% below a plasma frequency $\omega_p = 6000\text{ cm}^{-1}$ [93]. No plasma edge is observed at any temperature when the light is polarized along the b -direction [88, 93]. In terms of $\sigma(\omega)$, an insulating behavior is observed with an optical gap of $\approx 800\text{ cm}^{-1}$ in $(\text{TMTTF})_2\text{PF}_6$. The conductivity above the optical gap of 800 cm^{-1} contains almost all the spectral weight corresponding to $\omega_p = 6000\text{ cm}^{-1}$ namely, the sum rule condition

$$\int_{800}^{\infty} \sigma(\omega) d\omega = \omega_p^2/8,$$

is apparently well satisfied [93].

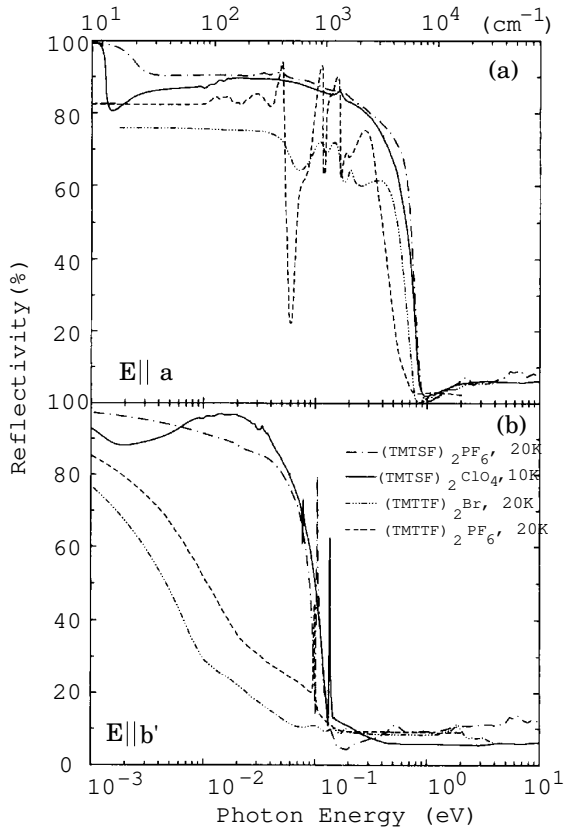


Figure 19: Optical reflectivity measurements for electric field parallel (a) and perpendicular to chains (b). After ref. [93].

Photoemission.— In experiments such as the angular resolved photoemission spectroscopy (ARPES), one has direct access to the momentum and energy dependent one-particle spectral density

$$A(\mathbf{k}, \omega) = \text{Im}G(\mathbf{k}, \omega), \quad (15)$$

which is defined as the imaginary part of the one-particle Green function $G(\mathbf{k}, \omega)$ [99]. In a Fermi liquid for example, $A(\mathbf{k}, \omega)$ is the probability that at a given energy ω , it exists a quasi-particle state at $\epsilon(\mathbf{k})$. It then expected to show a dispersing peak at $\omega = \epsilon(\mathbf{k})$, whose width equals $\tau_{\mathbf{k}}^{-1}$ and goes in principle to zero at $T = 0\text{K}$ — albeit in practice, it is limited to the experimental resolution in energy. For a Fermi liquid, $A(\mathbf{k}_F, \omega = \mu)$ should be finite at the Fermi level. So far, however, photoemission experiments have failed to detect any sign of quasi-particle states in both $(\text{TMTSF})_2\text{X}$ and $(\text{TMTTF})_2\text{X}$ series [100, 99].

The first photoemission experiments were made by Dardel *et al.* [100], on $(\text{TMTSF})_2\text{PF}_6$ at 50 K and the results were quite puzzling since no quasi-particle weight in the momentum-integrated intensity $\text{ImTr}_{k_a}G(\mathbf{k}, \omega)$ was found at the Fermi edge - this quantity corresponds to the density of states. Further the photoemission signal raises as a power of the energy from the Fermi edge and forms a broad but non-dispersing peak centered at a high energy of about 1 eV below E_F . These anomalous features of the

ARPES spectra remain largely unexplained.

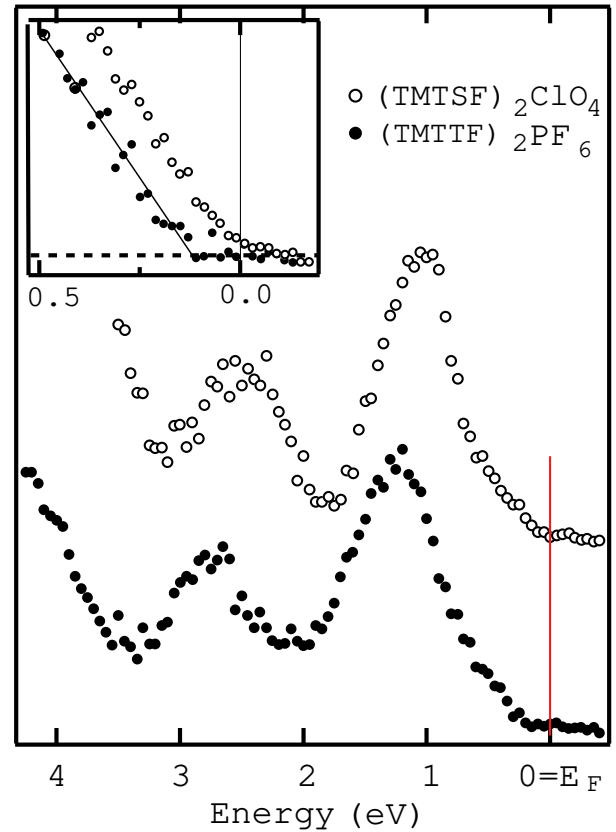


Figure 20: ARPES spectra of $(\text{TMTSF})_2\text{PF}_6$ and $(\text{TMTSF})_2\text{ClO}_4$ at Γ point (cf. Figure 6). The inset identifies an energy shift compatible with a charge gap in $(\text{TMTTF})_2\text{PF}_6$. After [99].

The ARPES spectra signal for the sulfur compound $(\text{TMTTF})_2\text{PF}_6$, displays a rigid shift of the leading edge near the Fermi energy to about 100 meV. This value is consistent with the charge gap of 900 K obtained from transport experiments DC or 800 cm^{-1} from optical conductivity of $(\text{TMTTF})_2\text{PF}_6$. Within a one-dimensional frame of interpretation, this gap has been ascribed to a Mott-Hubbard localization gap [99].

The Fermi liquid theory and the SDW instability.— Although the present review is not really concerned with the nature and the mechanisms of long-range ordering taking place in $(\text{TM})_2\text{X}$, these played, though indirectly, a relevant role when one tries to assess the viability of the Fermi liquid theory in spin-density-wave systems like the $(\text{TMTSF})_2\text{X}$. Following the example of the success of the BCS mechanism to explain the onset of conventional superconductivity as an instability of a Fermi liquid, there are many features of the spin-density-wave phase transition either in $(\text{TMTSF})_2\text{X}$ at low pressure or in $(\text{TMTTF})_2\text{X}$ at high pressure that can be fittingly described assuming the existence of a well defined Fermi liquid component in the normal phase. This can be substantiated if one looks at the mechanism of suppression of antiferromagnetism under pressure in the Bechgaard

salts (Figure 5) [38, 101]. It is generally held that the rapid drop of the SDW T_c under pressure (Figure 5) results from the gradual frustration of a particular symmetry property of the electronic spectrum – the so-called nesting. For an open Fermi surface as in the Figure 6 or the one resulting from the spectrum (2), perfect nesting conditions prevail so that electron and hole states on opposite sides of the Fermi surface are connected through the relation

$$\epsilon_p(\mathbf{k}) = -\epsilon_{-p}(\mathbf{k} + \mathbf{Q}_0), \quad (16)$$

where $\mathbf{Q}_0 = (2k_F^0, q_\perp^0)$ is the nesting vector that perfectly maps one part of the Fermi surface on the other.

Accordingly, the electron gas develops a singular logarithmic response

$$\begin{aligned} \Pi^0(\mathbf{Q}_0) &\sim \sum_{\mathbf{k}} \frac{n[\epsilon_p(\mathbf{k})] - n[\epsilon_{-p}(\mathbf{k} + \mathbf{Q}_0)]}{\epsilon_p(\mathbf{k}) - \epsilon_{-p}(\mathbf{k} + \mathbf{Q}_0)} \\ &\sim N(E_F^*) \ln \frac{E_x^0}{T}, \end{aligned} \quad (17)$$

to the electron-hole pair or density-wave formation at \mathbf{Q}_0 , where E_x^0 is a cut-off energy. A repulsive electron-electron coupling λ leads to an effective attraction between an electron and a hole separated by \mathbf{Q}_0 . The coupling to the singular electron gas response through a ladder diagrammatic summation will then predict an instability of the normal state – preferentially of the spin-density-wave type – when $g\Pi^0 \sim 1$, that is for

$$T_c \sim E_x^0 e^{-2/\lambda}. \quad (18)$$

In practice, however, the electron-hole symmetry relation (16) is never perfectly satisfied. There are deviations due to small corrections neglected in the spectrum (2). Following a lattice compression, the electron spectrum is altered and these deviations magnify under pressure and tend to suppress the logarithmic singularity (17); T_c thus rapidly decreases and even vanishes above some critical pressure (Fig. 5).

A prerequisite which is at the heart of this nesting mechanism is the existence of a coherent Fermi liquid component in at least two spatial directions for temperatures below $E_x^0 \sim T_{x1}$. Actually, the possibility to single out the electron-hole scattering channel in the ladder summation rests on the existence of quasi-particles and a coherent 2D Fermi surface – in the same way as the electron-electron pairing channel is selected in the BCS theory of superconductors. Otherwise for $T > t_{\perp b}^*$, the system is effectively 1D in character and there is no possibility to select the electron-hole pairing channel. The electron system turns out not to be a Fermi liquid (see Section 4).

In the same vein, another example one can quote in support of a Fermi liquid component in the right-hand side of the phase diagram is the unequivocal success of a description ‘à la BCS’ of the field-induced-spin-density-wave state phenomena taking place at very low temperature in these compounds [102, 103, 104, 105, 106]. This instability of the normal phase occurs in the presence of nesting frustration. A magnetic field applied along the c direction, however, restricts the electron motion along the b direction and ‘one-dimensionalizes’ the kinetics of quasi-particles. Perfect but quantized nesting conditions are found to

be restored which lead above some threshold field to an instability of the Fermi liquid toward a cascade of spin-density-wave states.

4. The quasi-one-dimensional approach to the normal phase of the Bechgaard salts

The point of view according to which the influence of low-dimensional physics is much more expanded in the normal phase of Bechgaard salts corresponds to the situation where the scale T_{x1} for the coherence in the transverse one-particle motion is at much lower temperature and can even become irrelevant under particular conditions. This naturally compels to call upon one-dimensional models of interacting electrons whose low-energy properties are known to differ from those of a Fermi liquid.

4.1. Electron gas model

In order to bring out the essential features behind the Luttinger liquid state we consider the electron gas model [107]. This model is of course a crude simplification of the interacting electron structure that takes place in actual organic compounds. Being defined with a small number of parameters, the model is nevertheless generic of a different kind of an electronic state that might be relevant to the description of organic conductors.

The model is based at the outset from the observation that a 1D non-interacting Fermi gas with a two-point Fermi surface at $\pm k_F^0$ gives rise to two infrared logarithmic singularities in the response of the system to correlate pair of particles either in the electron-electron (Cooper) or in the $2k_F^0$ electron-hole (Peierls) scattering channel. These are of the form

$$\begin{aligned} \Pi^0 &\sim 2N(E_F) \int_T^{E_F} \frac{d\epsilon}{\epsilon(k) - m\epsilon(k')} \\ &\sim N(E_F) \ln \frac{E_F}{T}. \end{aligned} \quad (19)$$

The singularity, though similar for both types of pairing, results from a distinct symmetry property of the one-particle spectrum. Take for example the logarithmic integration of the Cooper channel where $m = -1$ and $k' = -k$; it expresses the formation of pairs of particles of total momentum zero for which $\epsilon(k) = \epsilon(-k)$ is satisfied for the particles of each pair. In three dimensions, the slightest attraction between electrons in these time-reversed states inevitably leads to an instability of the metallic state towards BCS type of superconductivity. In one dimension, however, this singularity is not alone since the electron spectrum displays another type of symmetry property called ‘nesting’ for which $m = 1$ and $k' = k - 2k_F^0$, where this time the energies of an electron (or a hole) state at k and a hole (or an electron) state at $k - 2k_F^0$ are connected through the relation $\epsilon(k) = -\epsilon(k - 2k_F^0)$ – the 1D analog of eq. (16). The summation over a macroscopic number of intermediate states that are connected by nesting is responsible for a logarithmic integration of the form (19). It is the underlying mechanism of the Peierls lattice instability when $2k_F^0$ electron-hole pairs are coupled to low-frequency phonons [14].

What thus really makes one dimension so peculiar resides in the fact that the symmetry of the spectrum for the

Cooper and Peierls instabilities refer to the same phase space of electronic states [108]. The two different kinds of pairing act as independent and simultaneous processes of the electron-electron scattering amplitude which interfere with and distort each other at all order of perturbation theory. What comes out of this interference is neither a BCS superconductor nor a Peierls/density-wave superstructure but a different instability of the Fermi liquid called a Luttinger liquid.

Following the example of a Fermi liquid, however, a selected emphasis is put on the electronic states close to the Fermi level where the argument E_F/T of the logarithm goes to infinity at $T \rightarrow 0$. In the framework of the electron gas model, this amounts to write the one-particle kinetic term of the Hamiltonian in the form

$$H_0 = \sum_{p,k,\sigma} \epsilon_p(k) a_{p,k,\sigma}^\dagger a_{p,k,\sigma}, \quad (20)$$

where $\epsilon_p(k) \simeq v_F(pk - k_F^0)$ is linearized around the two Fermi points pk_F^0 for right $p = +$ and left $p = -$ moving electrons (a similar continuum approximation neglecting the details at short distance has been made in the context of the Fermi liquid theory [cf. Eq.(2)]).

Accordingly, direct interactions between carriers in the model can be defined close to the Fermi points, a procedure called the ‘g-ology’ decomposition of the interaction [107, 109]. For a rotationally invariant system, it allows to single out four different coupling constants: the backscattering and the forward scattering terms g_1 and g_2 , for which two electrons near opposite Fermi points are coupled through a momentum transfer near $2k_F^0$ and zero, respectively; the g_3 coupling corresponds to Umklapp scattering where two electrons near $+k_F^0$ (resp. $-k_F^0$) are backscattered to $-k_F^0$ (resp. $+k_F^0$), a process that is made possible at half-filling if the reciprocal lattice vector $G = 4k_F^0 = 2\pi/a$ enters in the momentum conservation law; finally, one has the coupling g_4 by which two electrons near k_F^0 (resp. $-k_F^0$) experience a small momentum transfer which keeps them on the same branch [109] (Figure 21).

Focusing for the moment on the most important couplings g_1 , g_2 and g_3 , the interacting part H_I of the total Hamiltonian can be written in the form

$$\begin{aligned} H_I = & (2g_2 - g_1) \sum_{p,q} \rho_p(q) \rho_{-p}(-q) - g_1 \sum_{p,q} \mathbf{S}_p(q) \cdot \mathbf{S}_{-p}(-q) \\ & + \frac{1}{2L} \sum_{\{p,k,Q,\sigma\}} g_3 a_{p,k_1+pQ,\sigma}^\dagger a_{p,k_2-pQ+pG,\sigma'}^\dagger a_{-p,k_2,\sigma'} a_{-p,k_1,\sigma}, \end{aligned} \quad (21)$$

where

$$\rho_p(q) = \frac{1}{2}(L)^{-\frac{1}{2}} \sum_{\{k,\alpha\}} a_{p,\alpha}^\dagger(k+q) a_{p,\alpha}(k),$$

and

$$\mathbf{S}_p(q) = \frac{1}{2}(L)^{-\frac{1}{2}} \sum_{\{k,\alpha\beta\}} a_{p,\alpha}^\dagger(k+q) \vec{\sigma}^{\alpha\beta} a_{p,\beta}(k),$$

are respectively the long wavelength charge- and spin-density operators for right- or left-moving carriers.

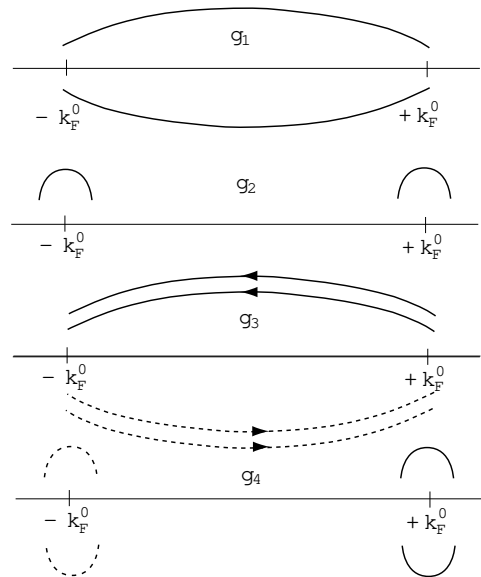


Figure 21: g-ology decomposition of the electron-electron interaction close to the Fermi points $\pm k_F^0$ in the electron gas model.

The connection of the effective intrachain g-ology couplings with the intramolecular or one-site repulsive interaction and the screened long-range Coulomb matrix element have been discussed in detail by Barisic *et al.* [110, 111, 112]. For g_1 , g_2 and g_3 , one has the following result

$$\begin{aligned} g_1 & \approx Ua, \\ g_2 & \approx Ua + 2Va \left(\ln \frac{E_F}{\omega_p} + 1 \right), \end{aligned} \quad (22)$$

where ω_p is the plasma frequency and V is the Coulomb matrix element between neighboring molecular sites. The screening – here non-logarithmic – of the long range part of the Coulomb interaction thus appears in the renormalization of the forward scattering amplitude. As for the Umklapp term g_3 , if one refers exclusively to the amplitude of the dimerization in the evaluation of the half-filled character of the band [113, 101, 114], one finds in the lowest order

$$g_3 \approx g_1 \frac{\Delta_D}{E_F}, \quad (23)$$

where Δ_D is the dimerization gap at $\pm 2k_F^0$. This expression does not account, however, for the full influence of the anion lattice on the amplitude of Umklapp scattering [115, 50]. Although a $4k_F^0$ anion potential in the presence of an infinitely rigid lattice produces no dimerization, the $4k_F^0$ bond-charge modulation induced by the anions subsists, however, and is sufficient to enhance Umklapp scattering. The expression (23) can thus be considered as a lower bound to the actual bare value of g_3 in the Bechgaard salts [50].

It is worth noting that the electron gas model is a continuum model which is valid at low energy, so the connection with the parameters U and V of the lattice model can only be considered as approximate. For example, in the high-temperature range or for sufficiently large couplings the curvature of the band may become relevant and it is

not clear if a continuum theory will work well quantitatively [116, 117]. The point at issue is the ‘input’ parameters of the electron gas model. These are likely to enter in the theory as screened quantities due to non-logarithmic many-body effects and they should then differ from the bare parameters of the lattice model.

4.2. Scaling theory

A simple feature of logarithmic divergences like (19) is the lack of a particular scale in the energy interval between E_F and T . Another way to put it is to say that there is *scale invariance* since each part of the integral in (19), whatever its size inside the interval, gives a logarithmic contribution that is independent of either T or E_F [60]. Scaling that is present at the lowest order will carry over not only to leading, but also to next-to-leading, etc., logarithmic singularities of the scattering amplitudes. Therefore the perturbation theory and in its turn the properties of the electron gas model as a whole will become scale invariant.

The renormalization group method is an appropriate device to sum up perturbative series of this sort. Schematizing the basic idea behind this procedure, it consists of the successive partial integrations of outer energy-shell band electron states in the partition function Z [118, 91, 109]. Consequent to this reduction of electronic degrees of freedom, the Hamiltonian keeps the same form except for the scaling or the renormalization of the coupling constants. Other static and dynamical quantities that can be worked out using Z such as the response functions, the one-particle spectral weight, the density of states, etc., will also show renormalization. The recursion relation of the hamiltonian in Z is meant by the following transformation

$$Z = \text{Tr}_{<} \text{Tr}_{\text{o.s.}} e^{-\beta H} \propto \text{Tr}_{<} e^{-\beta H_{d\ell}} \dots \propto \text{Tr}_{<} \text{Tr}_{\text{o.s.}} e^{-\beta H_\ell} \propto \text{Tr}_{<} e^{-\beta H_{\ell+d\ell}}, \quad (24)$$

where $\text{Tr}_{\text{o.s.}}$ is the partial sum of diagonal matrix elements in a outer energy shell $\frac{1}{2}E_0(\ell)d\ell$ on both sides of the Fermi level. Here $d\ell$ is the infinitesimal generator for the bandwidth reduction $E_0(\ell) \rightarrow E_0(\ell + d\ell) = E_0(\ell)e^{-d\ell}$ and $E_0(\ell) = 2E_F e^{-\ell}$ corresponds to the effective or scaled bandwidth at the step ℓ . Under the renormalization group transformation

$$\mathcal{R}_{d\ell}[H_\ell] = H_{\ell+d\ell},$$

the flow of coupling constants results at one-loop level from the Peierls and Cooper logarithmic divergences. These differ in sign and lead to important cancellations (interference) in the renormalization flow [107]. Thus, after all possible cancellations being made, the flow is found to be governed by the following set of equations

$$\begin{aligned} \frac{d\tilde{g}_1}{d\ell} &= -\tilde{g}_1^2 + N_1, \\ \frac{d(2\tilde{g}_2 - \tilde{g}_1)}{d\ell} &= \tilde{g}_3^2 + N_2, \\ \frac{d\tilde{g}_3}{d\ell} &= \tilde{g}_3(2\tilde{g}_2 - \tilde{g}_1) + N_3. \end{aligned} \quad (25)$$

Here we have defined $\tilde{g}_1 \equiv g_1/\pi v_\sigma$, $(2\tilde{g}_2 - \tilde{g}_1) \equiv (2g_2 - g_1)/\pi v_\rho$, and $\tilde{g}_3 = g_3/\pi v_\rho$, by introducing the renormalization of the velocities

$$v_{\rho,\sigma} = v_F[1 \pm g_4/(2\pi v_F)].$$

The terms $N_{i=1,2,3} \sim \mathcal{O}(\tilde{g}^3)$ give the higher order (two-loop) contributions.

What immediately comes out of these equations at the one-loop level is the fact that $g_1(\ell)$ is decoupled from the set of couplings $(2g_2 - g_1)(\ell)$ and $g_3(\ell)$. Reverting to the expression (21) for the Hamiltonian, this means that long-wavelength charge and spin correlations are decoupled, a key feature of a Luttinger liquid known as *spin-charge separation*.

Consider the charge part, the flow moves along hyperbolas defined by the equation (invariant) $(2\tilde{g}_2 - \tilde{g}_1)^2 - \tilde{g}_3^2 = C$ (Figure 22). Therefore for $g_1 - 2g_2 < |g_3|$, it drives both g_3 and $2g_2 - g_1$ to strong coupling where a singularity develops in the charge sector at $\ell_\rho \equiv \ln E_F/T_\rho$, corresponding to the temperature scale

$$T_\rho = E_F e^{-1/\sqrt{C}}. \quad (26)$$

This signals the presence of a *gap* $\Delta_\rho \sim T_\rho$ in the charge degrees of freedom, which has the same origin as the Mott-Hubbard gap in the one-dimensional Hubbard model at half-filling [119].

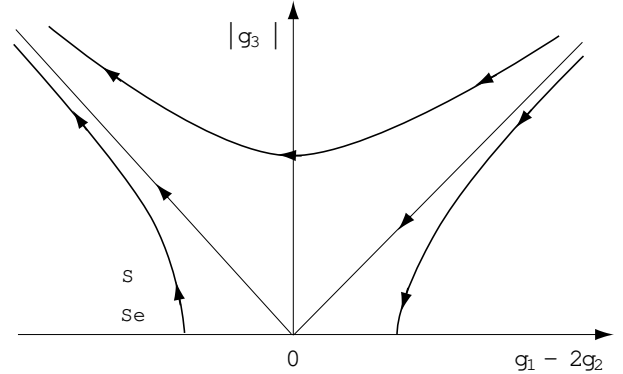


Figure 22: Renormalization group flow of the couplings in the charge sector. The points S and Se indicate locations of members of the $(\text{TMTTF})_2\text{X}$ and $(\text{TMTSF})_2\text{X}$ series.

As for the spin part it is governed by the flow of g_1 and at the one-loop level, one finds at once

$$g_1(\ell) = \frac{g_1}{1 + (\pi v_\sigma)^{-1} g_1 \ell}. \quad (27)$$

The case of practical interest is a repulsive $g_1 > 0$, where $g_1(\ell \rightarrow \infty) \rightarrow 0$, and which becomes marginally irrelevant. Thus referring to the expressions (22) and (23), which should hold for the Bechgaard salts and their sulfur analogs, the domain of interest for these systems would be located on the left-hand-side of the flow diagram in Figure 22. In this scenario, the properties of $(\text{TMTSF})_2\text{X}$ and $(\text{TMTTF})_2\text{X}$, should scale towards those of the purely one-dimensional Hubbard model at half-filling which shows an insulating state and gapless spins degrees of freedom.

At the two-loop level, the recursion relations for the couplings are obtained using the expressions [120]:

$$N_1 = -\frac{1}{2}\tilde{g}_1^3,$$

$$N_2 = -\frac{1}{2}\tilde{g}_3^2(2\tilde{g}_2 - \tilde{g}_1),$$

$$N_3 = -\frac{1}{4}\tilde{g}_3(2\tilde{g}_2 - \tilde{g}_1)^2 - \frac{1}{4}\tilde{g}_3^3.$$

Spin-charge separation is preserved and the singularity at T_ρ , albeit removed for g_3 and $2g_2 - g_1$, is replaced as $\ell \rightarrow \infty$ by a strong coupling fixed point at $g_3^* \rightarrow 2\pi v_\rho$, $g_2^* \rightarrow \pi v_\rho$ and $g_1^* \rightarrow 0$, which is still indicative of a gap Δ_ρ in the charge.

Scattering time and transport.— A rapid growth of Umklapp scattering as T_ρ is approached from above carries with it dissipation of momentum which increases resistivity. The two-loop evaluation of the imaginary part of the self-energy in the one-particle Green function leads to the following expression for the 1D electron-electron scattering rate as a function of temperature [121]:

$$\tau^{-1} \sim [g_3(T)]^2 T. \quad (28)$$

The insulating behavior of $(\text{TMTTF})_2\text{X}$ and $(\text{TMDTDSF})_2\text{X}$ as the temperature is decreased in the normal phase (Figure 4) has been ascribed to the presence of T_ρ and to the relevance of one-dimensional Umklapp scattering in these materials [115, 122, 123]. As the temperature is lowered, however, the increase of g_3 is faster than the phase space factor $1/T$ so that a metallic phase should be absent at all temperature which is not corroborated by experiments (Figure 4). This result is confirmed by more elaborate calculations [124]. It was pointed out that in systems like $(\text{TMTSF})_2\text{X}$ and $(\text{TMTTF})_2\text{X}$, g_3 is not the only source of Umklapp scattering [96]. Actually in the temperature range where $T > \Delta_D$, the influence of dimerization is small and the hole band becomes essentially 3/4-filled (or 1/4-filled for an electron band) which introduces an Umklapp term that is specific to this order of commensurability. The quarter-filling Umklapp term noted $g_{1/4}$ will give rise to an additional scattering channel for the carriers which allows to write the total electron-electron scattering rate as the sum of two contributions:

$$\tau^{-1} = \tau_{g_3}^{-1} + \tau_{g_{1/4}}^{-1}. \quad (29)$$

Here $\tau_{g_{1/4}}^{-1}$ is expected to be the dominant contribution at high enough temperature and since the growth of $g_{1/4}(T)$ is less rapid than for $g_3(T)$ as one moves down in temperature, this would give rise to a metallic behavior over a sizable domain of the normal phase. Although the $g_{1/4}$ term could be introduced in the above renormalization group approach, its influence on the scattering rate will be rather discussed in more details in the context of the bosonization method.

Spin susceptibility.— The absence of any anomaly in the spin susceptibility near T_ρ and its temperature variation can also be accounted for in the one-dimensional picture. According to (27) and (21), the spins remain gapless for $g_1 > 0$ but the logarithmic screening of g_1 introduces a scale dependent exchange coupling between left and right spin densities, which in its turn, affects the temperature variation of the spin susceptibility. Since within the electron gas model, long wavelength spin-density excitations are non-interacting modes, these can be appropriately described

within a RPA type of calculation [68], which yields

$$\chi_s(T) = \frac{2\mu_B^2(\pi v_\sigma)^{-1}}{1 - (2\pi v_\sigma)^{-1}g_1(T)}. \quad (30)$$

This expression for the susceptibility is of interest in many respects. One first verifies that as $T \rightarrow 0$, $g_1(T) \rightarrow 0$ and $\chi_s \rightarrow 2\mu_B^2(\pi v_\sigma)^{-1}$, a result that agrees with the exact result of Shiba for the Hubbard model at small U [125]. The enhancement then differs from the unrenormalized Hartree-Fock theory (3), for which the logarithmic screening of g_1 is absent and where $F^a = \frac{1}{2}N(E_F)(g_1 + g_4)$ is larger in amplitude. Secondly, owing to the logarithmic screening of the backward scattering, the susceptibility shows a temperature variation that can be made congruent with observation made for both $(\text{TMTTF})_2\text{X}$ and $(\text{TMTSF})_2\text{X}$ series [58]. Take for example the case of $(\text{TMTSF})_2\text{X}$; when χ_s data are corrected for thermal dilatation and restored to their constant volume values, the amplitude of χ_s at 300 K is found to be about 30% larger than at 50 K, below which it becomes essentially flat in temperature. As shown by Wzietek *et al.* [58], by taking in the Hubbard limit $g_1 = g_4 = aU \sim \pi v_F$ and typical band calculation values $E_F \sim 3000\text{K}$ for the Fermi energy, quite reasonable agreement can be obtained between the predicted and the observed temperature variations of χ_s in this temperature interval. The same type of analysis carries over to $(\text{TMTTF})_2\text{X}$ compounds [126, 127], where similar figures for the electron coupling constants and the use of somewhat lower values of E_F lead to similar agreement [58]. In this frame then, the temperature variation of the susceptibility in the normal phase can provide useful information on the range of one-dimensional physics in these materials.

One-particle spectral properties.— The two-loop corrections are also of interest for the quasi-particle weight z (cf. Eq. 7) at the Fermi level which is governed by the scaling equation

$$\frac{d}{d\ell} \ln z = -\frac{1}{16}[C + \frac{3}{4}(\tilde{g}_1^2 + \tilde{g}_3^2)]. \quad (31)$$

The integration leads to the power law decay

$$z(x) \sim x^\alpha, \quad (32)$$

where x can be identified either with ω (for $T = 0$) or T (for $\omega < T$). As for the power law exponent α , it is positive and in general non-universal indicating that at zero temperature there are no quasi-particle states at the Fermi level, a characteristic feature of the Luttinger liquid. The spectral function is

$$\text{Im } G_p(k_F^0, \omega) \sim |\omega|^{\alpha-1}, \quad (33)$$

which also varies as a power of the energy.

Attempts to interpret ARPES data of $(\text{TMTSF})_2\text{X}$ in the normal metallic phase by using a power law behavior of this form for the spectral weight have shown to require rather large values of α [100], which are not accessible through the above perturbative renormalization group method. Away from the strong coupling fixed point, the present approach predicts that α is a rather small quantity in the metallic phase. More elaborate calculations like the bosonization technique (see below) and numerical calculations allow to give a more precise treatment of the exponents of spectral functions at low energy [128, 129, 130].

Response functions.— The elementary Cooper and Peierls logarithmic divergences (19) of the interacting electron gas are also present order by order in the perturbation theory of response functions in the $2k_F^0$ density-wave and superconducting channels. A scaling procedure can thus be applied in order to obtain the asymptotic properties of the real part of the retarded response functions which we will note $\chi_\mu(\ell)$. It is convenient to introduce auxiliary response functions noted $\bar{\chi}_\mu(\ell)$ [107], which are defined

$$\chi_\mu(\ell) = -(\pi v_F)^{-1} \int_0^\ell \bar{\chi}_\mu(\ell') d\ell'. \quad (34)$$

In the presence of Umklapp scattering, the following susceptibilities will be considered: for the Peierls channel at $2k_F^0$, one has the ‘on-site’ $\mu = \text{SDW}$ for spin-density-wave and $\mu = \text{BOW}$ for the ‘bond-order-wave’; in the Cooper channel, one has singlet $\mu = \text{SS}$ and triplet $\mu = \text{TS}$ superconducting correlations. At two-loop level, the auxiliary responses are governed by the flow equations

$$\frac{d}{d\ell} \ln \bar{\chi}_\mu = g_\mu(\ell) + \frac{1}{2} [g_1^2(\ell) + g_2^2(\ell) - g_1(\ell)g_2(\ell) + \frac{1}{2}g_3^2(\ell)], \quad (35)$$

where $g_{\text{SDW}} = g_2(\ell) + g_3(\ell)$ and $g_{\text{BOW}} = g_2(\ell) + g_3(\ell) - 2g_1(\ell)$ for the Peierls channel; and $g_{\text{SS}} = -g_1(\ell) - g_2(\ell)$, and $g_{\text{TS}} = -g_2(\ell) + g_1(\ell)$ for the Cooper channel. In the repulsive sector which is of interest for the Bechgaard salts, only SDW and BOW correlations develop singular responses² at $2k_F^0$ (Figure 23). Using (25), the asymptotic behavior of the auxiliary response as a function of temperature is found to be

$$\bar{\chi}_\mu(T) \approx X_\mu(E_F/\Delta_\rho) \left(\frac{\Delta_\rho}{T}\right)^{-\gamma_\mu^*}, \quad (36)$$

which varies as a power of the temperature. In the presence of a Mott-Hubbard gap, the exponent for both bond-order-wave and site spin-density-wave $\gamma_{\text{SDW}}^* = \gamma_{\text{BOW}}^* = 3/2$ are then of the order of unity. Here X_μ are scaling factors that give the power law behavior in the weak coupling domain, where g_3 is weak and γ_μ is smaller than unity. The possible singularities of the electron gas at half-filling are summarized in Figure 23.

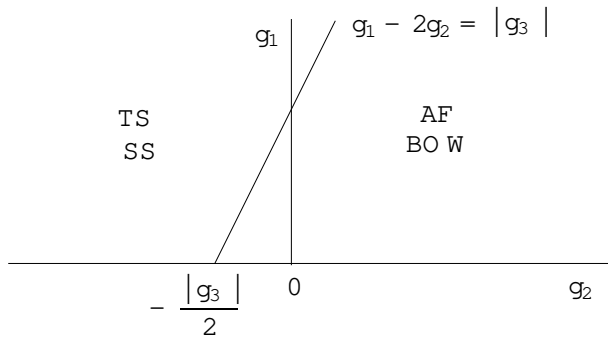


Figure 23: Phase diagram of the electron gas model in the repulsive sector ($g_1 > 0$) and in presence of Umklapp scattering.

²Here we do not consider the $4k_F^0$ response of the electron gas which is also singular in this sector [131].

These results of the one-dimensional theory are of interest since they indicate that the relevance of Umklapp processes at half-filling eliminates the possibility of charge-density-wave correlations which usually drive an incommensurate system to a Peierls instability – as it is the case for TTF-TCNQ [115]. Instead of a Peierls instability, antiferromagnetic correlations dominate. This is consistent with the fact that antiferromagnetism plays a very important part of the phase diagram of $(\text{TM})_2\text{X}$ (Figure 5). Bond-order-wave correlations, however, subsist according to the renormalization group results – on almost equal footing with antiferromagnetism. For dimerized TMTTF or TMTSF stacks, these would correspond to the correlation of the carrier tunneling across the ‘bond’ separating each dimer at wave vector $2k_F^0$. When the coupling of these electronic correlations to acoustic phonons is suitable, the system has the possibility to develop a structural instability called a spin-Peierls instability, which is the analog of the Peierls distortion when the electronic part of the system is Mott-Hubbard insulating instead of metallic away from half-filling.

One-dimensional precursors to a spin-Peierls instability has been clearly identified by X-ray diffuse scattering experiments in $(\text{TMTTF})_2\text{PF}_6$, $(\text{TMTTF})_2\text{AsF}_6$ and $(\text{TMDTDSF})_2\text{PF}_6$, well above the transition temperature and for low pressure conditions (Figure 24). As one moves to the right-hand-side of the phase diagram in Figure 5, these precursor effects of the normal phase dwindle in amplitude. In $(\text{TMTSF})_2\text{PF}_6$ for example, where the normal phase is metallic and Umklapp processes are less singular, $2k_F^0$ X-ray diffuse scattering is small in amplitude and shows a slow increase as a function of temperature down to 50K, below which it starts decreasing [132, 42, 133]. These X-ray features convey in a way the strength of the one-dimensional bond-order-wave singularity in the electronic system, which turns out to be consistent with the prediction of the one-dimensional theory. Indeed, the explicit evaluation of the amplitude of the scaling factor $X_{\text{BOW}}(T) \ll X_{\text{SDW}}(T)$ – in the absence of a charge gap – is found to be much smaller for BOW than for antiferromagnetism. It is worth emphasizing that although such lattice precursors are weak in amplitude in systems like $(\text{TMTSF})_2\text{X}$, they have the same one-dimensional character as in $(\text{TMTTF})_2\text{PF}_6$, or in Peierls systems like TTF-TCNQ [134] and KCP [135]. Therefore the temperature profile of the X-ray diffuse scattering intensity (Figure 24) can be seen as a precious indication about the extent to which one-dimensional physics is relevant in the normal phase of these systems.

4.3. The concept of Luttinger liquid and bosonization

In the presence of strong coupling for the charge couplings g_3 and $2g_2 - g_1$, the renormalization group approach, which relies on the perturbation theory of original fermions, becomes less accurate in obtaining quantities like the power law indexes. For more quantitative results, it is therefore suitable to call on a different approach which can even allow in some special cases an exact solution of the problem. In what follows we would like to give a brief presentation of the relevant results that can be obtained by the bosonization approach and how this supplementary amount of information can help to go deeper in our understanding of the normal phase of the Bechgaard salts and their sulfur analogs.

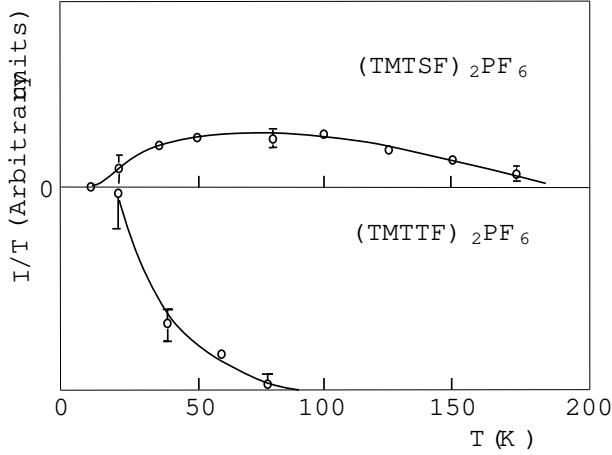


Figure 24: Temperature dependence of the $2k_F^0$ scattering intensities for (TMTSF) $_2$ PF $_6$ (top) and (TMTTF) $_2$ PF $_6$ (bottom) in the normal phase, after [42].

A feature of peculiar importance in one dimension is that long wavelength charge or spin-density-wave oscillations constructed by the combination of electron-hole pair excitations at low energy form extremely stable excitations [128]. These actually have no available phase space to decay – in contrast to the situation found in a Fermi liquid where a damping exists [52]. Quasi-particles are absent at low energy for a one-dimensional system of interacting electrons and are replaced by collective acoustic excitations for both spin and charge degrees and freedom which turn out to be the true eigenstates of the system [128]. Following the example of Debye sound waves in a one-dimensional solid, their dispersion relations are linear and reads

$$\omega_{\sigma,\rho} = u_{\sigma,\rho} |q|. \quad (37)$$

where $u_{\sigma,\rho}$ is the velocity of each of these modes. Collective oscillations of the electron gas will then obey boson statistics and the connection between the original Fermi and boson fields is made possible through the following relation

$$\psi_{p,\sigma}(x) = L^{-\frac{1}{2}} \sum_k a_{p,k,\sigma} e^{ikx} \sim \lim_{\alpha_0 \rightarrow 0} \frac{e^{ipk_F^0 x}}{\sqrt{2\pi\alpha_0}} \exp\left(-\frac{i}{\sqrt{2}}[p(\phi_\rho + \sigma\phi_\sigma) + (\theta_\rho + \sigma\theta_\sigma)]\right), \quad (38)$$

where the spin and charge phase fields $\phi_{\rho,\sigma}$ have been introduced [136]. These satisfy the commutation relation

$$[\Pi_{\nu'}(x'), \phi_\nu(x)] = -i\delta_{\nu\nu'}\delta(x-x'), \quad (39)$$

where $\Pi_\nu(x)$ is the momentum conjugate to $\phi_\nu(x)$ and is defined by $\theta_\nu(x) = \pi \int \Pi_\nu(x') dx'$. Following Schulz *et al.* [136], the phase variable representation allows to rewrite the full electron gas Hamiltonian in the form

$$H = \sum_{\nu=\rho,\sigma} \frac{1}{2} \int \left[\pi u_\nu K_\nu \Pi_\nu^2 + u_\nu (\pi K_\nu)^{-1} \left(\frac{\partial \phi_\nu}{\partial x} \right)^2 \right] dx + \frac{2g_1}{(2\pi\alpha_0)^2} \int \cos(\sqrt{8}\phi_\sigma) dx$$

$$+ \frac{2g_3}{(2\pi\alpha_0)^2} \int \cos(\sqrt{8}\phi_\rho) dx + \frac{2g_{1/4}}{(2\pi\alpha_0)^2} \int \cos(2\sqrt{8}\phi_\rho) dx. \quad (40)$$

The harmonic part of the phase Hamiltonian corresponds to the Tomonaga-Luttinger model with no backscattering and Umklapp terms. It is exactly solvable, the spectrum shows only collective excitations and all the properties of the model then become entirely governed by the velocity u_ν and the ‘stiffness constant’ K_ν of acoustic excitations, which are functions of the microscopic coupling constants and differ for the charge and spin. The collective modes for the spin and charge are decoupled and this leads to spin-charge separation of the Luttinger liquid. When backscattering or/and Umklapp scattering are non zero, the sine-Gordon terms in (40) do not allow an exact solution in general – except for particular values of couplings corresponding to the Luther-Emery model [137, 138]. Note that in (40), the contribution coming from quarter-filling Umklapp processes has been added to the phase Hamiltonian [96]. This source of Umklapp scattering should dominate in the temperature domain where $T \gg \Delta_D$ and the influence of dimerization gap should be small. In the Hubbard limit, its bare amplitude is given by

$$g_{1/4} \approx aE_0 \left(\frac{U}{E_0} \right)^3. \quad (41)$$

Renormalization group method can be used to determine the flow of renormalization for $(g_1, g_3, g_{1/4})$ when these act as perturbations for the Luttinger liquid parameters (K_ν, u_ν) as a function of energy.

The properties of the model in the repulsive sector can be obtained at low energy by looking close to the fixed point. For a rotationally invariant system at half-filling or quarter-filling, one gets $g_1^* \rightarrow 0$, while $g_3^*(g_{1/4}^*)$ and $2g_2^* - g_1^*$ reach strong coupling. In this case, one has

$$K_\sigma^* \rightarrow 1, \quad u_\sigma^* \rightarrow v_\sigma \quad K_\rho^* \rightarrow 0, \quad u_\rho^* \rightarrow (2\pi)^{-1} \sqrt{(2\pi v_\rho)^2 - (2g_2^* - g_1^*)^2}, \quad (42)$$

which implies a vanishing velocity for collective charge excitations and a gap given by

$$\Delta_\rho \sim E_0 \left(\frac{gU}{E_0} \right)^{1/[2(1-n^2 K_\rho)]}, \quad (43)$$

where $n = 1$ for $gU = g_3$, and $n = 2$ for $gU = g_{1/4}$ at half-filling and quarter-filling, respectively. It should be stressed here that in the pure quarter-filled (resp. half-filled) case, the existence of a charge gap is subjected to the condition $K_\rho < .25$ (resp. $K_\rho < 1$) – here $K_\rho = 1$ refers to free electrons [130]. In the metallic range where g_3 and $2g_2 - g_1$ are not too large, K_ρ and u_ρ are finite, while one can take $K_\sigma = 1$ for the spin part if the system is invariant under rotation. The Luttinger liquid parameters u_ρ , K_ρ and u_σ at low energy can also be obtained using numerical methods applied to lattice models at different band fillings [129, 130].

Given the values of the Luttinger liquid parameters, we can now look at the properties of the system using the harmonic part of the Hamiltonian. Thus the spin-spin correlation function at $2k_F^0$ can be expressed as statistical

averages over phase variables, which can be explicitly evaluated [136, 128]. At equal-time for example, one gets – after dropping logarithmic corrections – the power law decay

$$\chi(x) = (\mathbf{S}(x) \cdot \mathbf{S}(0)) \sim \frac{\cos(2k_F^0 x)}{x^{1+K_\rho}}. \quad (44)$$

The stiffness constant K_ρ then entirely governs the algebraic decay of the antiferromagnetic correlations. The spin response at $2k_F^0$ is given by

$$\chi(2k_F^0, T) \sim T^{-1+K_\rho}. \quad (45)$$

The power law singularity is therefore the strongest in the presence of a charge-degrees-of-freedom gap where $K_\rho = 0$, which actually corresponds to the Heisenberg universality class.

Nuclear spin-lattice relaxation: insulating domain. – As mentioned earlier a good insight into spin correlations can be obtained through nuclear spin-lattice relaxation. According to (11), T_1^{-1} is related to the imaginary part of the dynamical spin response. In a Luttinger liquid $\text{Im}\chi(q, \omega \rightarrow 0)$ is strongly peaked at $q = 0$ and $2k_F^0$, so the integration over all modes makes both types of low-lying excitations contributing to the relaxation rate [67, 68].

Near $q = 0$, one finds for the spectral weight of spin excitations:

$$\text{Im}\chi(q, \omega) = \frac{1}{4v_\sigma} \sum_p \frac{pv_\sigma q \delta(\omega - pv_\sigma q)}{[1 - (2\pi v_\sigma)^{-1} g_1(T)]^2}. \quad (46)$$

The presence of a delta function in this expression indicates the absence of damping for paramagnons in a Luttinger liquid – in contrast to a Fermi liquid (see Eq. 9) – this also indicates that spin collective excitations are exact eigenstates of the system in one dimension (similar conclusions also hold for the charge part). Now close to $q = 2k_F^0$, one can use the following expression [118]:

$$\text{Im}\chi(q \sim 2k_F^0, \omega \rightarrow 0) \sim T^{-1+K_\rho} \omega, \quad (47)$$

which is valid in the low frequency limit. The summation over all q -vectors in the expression of the nuclear relaxation rate can then be evaluated at once and yields [68, 67]

$$T_1^{-1} = C_0 T \chi_s^2(T) + C_1 T^{K_\rho}, \quad (48)$$

where C_0 and C_1 are T -independent parameters. For a Luttinger liquid, the nuclear relaxation rate is thus enhanced with respect to the Korringa law. The temperature variation of the enhancement then combines two different contributions which leads to a characteristic temperature profile for the relaxation rate. In the high temperature domain, antiferromagnetic correlations are weak and the relaxation rate is dominated by the enhancement of the square of the spin susceptibility, which leads according to (30) to an upward curvature of T_1^{-1} as a function of T , while it is the other way round in the low temperature domain (see Figure 12); there, the contribution of paramagnons becomes smaller to the benefit of antiferromagnetic spin correlations which eventually merge as the dominant source of enhancement which varies as power of the temperature.

As previously mentioned, the exponent K_ρ is zero for a 1-D Mott-Hubbard insulator and antiferromagnetic spin fluctuations contribute a constant term to the relaxation rate. A canonical example for this behavior is observed in $(\text{TMTTF})_2\text{PF}_6$ [58], as T_1^{-1} plotted versus the measured value of $T\chi_s^2(T)$ shows a finite intercept at $T = 0$ (Fig. 25). Other illustrations for the viability of the 1-D model for spins are also given by systems such as $(\text{TMTTF})_2\text{Br}$ [58] and $(\text{TMDTDSF})_2\text{PF}_6$ [139], exhibiting a less pronounced Mott insulating character with T_ρ only in the 80 – 200 K range. T_1^{-1} follows a linear law without any finite intercept at low temperature as long as $T > T_\rho$ [140]. This is the expected behavior when the $q = 0$ fluctuations are predominant. Antiferromagnetic fluctuations show a much stronger singularity below T_ρ where $K_\rho = 0$ and contribute according to (48) an additional constant term to the relaxation at very low temperature (Fig. 25).

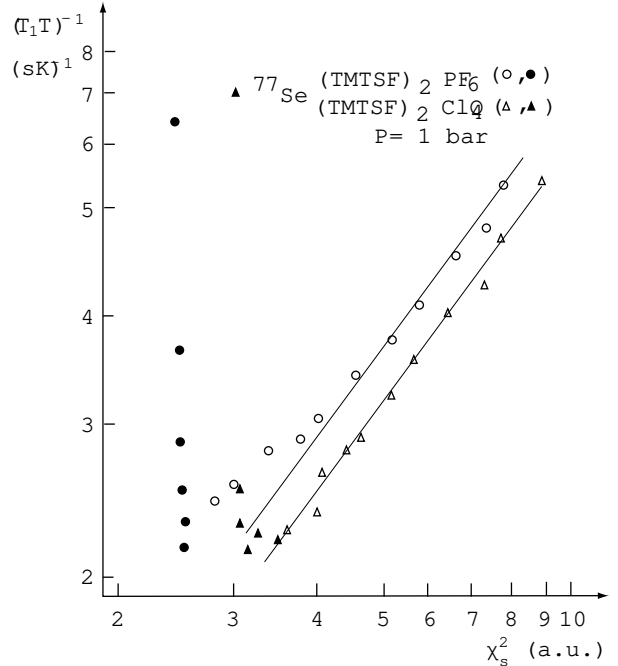


Figure 25: ^{13}C T_1^{-1} vs measured EPR $T\chi_s^2$ data for $(\text{TMTTF})_2\text{PF}_6$ and $(\text{TMTTF})_2\text{Br}$ (top); ^{77}Se T_1^{-1} vs measured Faraday $T\chi_s^2$ data for $(\text{TMTSF})_2\text{PF}_6$ (bottom), after [67, 58].

Antiferromagnetism ordering in the presence of a charge gap. – The intrastack charge localization resulting from the effect of Umklapp scattering is also accompanied by a confinement of the carriers on individual stacks. This confinement can be viewed as a result of a reduction in the transverse kinetic coupling $t_{\perp b}$ due to the correlations in the 1-D Mott state (i.e. the renormalization of the transverse crossover T_{x1} in one-particle motion discussed at the beginning of the section 3 on the Fermi liquid) to the extent of becoming completely irrelevant [123, 91]. In spite of the absence of a cross-over in the coherent single-particle motion, the existence of long-range antiferromagnetic order, which is known to be found in the range of 5–25K in

(TMTTF)₂X, indicates that spin correlations end in deconfinement at sufficiently low temperature. Following the example of localized spins in the Heisenberg limit, this is made possible through a kinetic exchange interaction $J_{\perp b}$ between spins of neighboring chains [123, 122, 91], which can also be viewed as the interchain transfer of bound electron-hole pairs. In Mott-Hubbard systems like (TMTTF)₂X, however, the localization of carriers is less pronounced than in the Heisenberg limit and virtual processes take place over larger distances $\xi_{\rho} \sim v_F/\Delta_{\rho} \gg a$, which magnifies the exchange to yield

$$J_{\perp, b} \approx \frac{\xi_{\rho} t_{\perp b}^{*2}}{a \Delta_{\rho}},$$

where $t_{\perp b}^*$ is the effective but finite interchain hopping taking place at the energy scale Δ_{ρ} . Interchain exchange is the key mechanism for promoting antiferromagnetic long range order in (TMTTF)₂X over a sizable range of pressure, and to a lesser extent in (TMTSF)₂X. By its coupling to singular antiferromagnetic fluctuations along the chains, the condition for the onset of critical ordering is given by $J_{\perp, b}\chi(2k_F^0, T_N) \sim 1$, which yields

$$T_N \sim \frac{t_{\perp b}^{*2}}{\Delta_{\rho}}.$$

This leads to a characteristic increase of T_N as a function of pressure which is observed experimentally [141, 84]. This lends additional support for the existence of a Luttinger liquid state severed of its charge component in the normal phase of these compounds (see Fig. 5).

Nuclear spin-lattice relaxation: conducting regime.— As for the spin sector in the conducting regime, an approach to the 1-D exponent K_{ρ} can be attempted looking at the spin-lattice relaxation rate for which the $2k_F^0$ contribution should become predominant at low temperature where $0 < K_{\rho} < 1$ and a deviation in the law $1/T_1 \sim T\chi_s^2(T)$ can be anticipated. This is precisely what is observed from the ⁷⁷Se-NMR in (TMTSF)₂PF₆, where the log-log plot of $(T_1 T)^{-1}$ versus $\chi_s^2(T)$ shows a deviation from linearity below 150K or so (Fig. 11), signaling the onset of $2k_F^0$ fluctuations. These AF fluctuations become even more visible when T_1^{-1} is plotted versus T for (TMTSF)₂ClO₄ as shown in Fig. 12 – or for (TMTSF)₂PF₆ under a pressure which is large enough to suppress the SDW ground state [58]. A temperature independent contribution arises below 50 – 30 K (i.e., much above the temperature regime for 3-D critical fluctuations). The non-critical enhancement of T_1^{-1} is thus too large to be ascribed to a Fermi liquid contribution which should behave linearly in a temperature regime where the spin susceptibility is constant (see eq. (12)). The comparison between the behavior of (TMTSF)₂PF₆ at low temperature and compounds such as (TMTTF)₂Br or (TMDTDSF)₂PF₆ which evolve towards the Mott insulator limit at low temperature shows that the strong coupling limit is not reached in case of selenium compounds, namely K_{ρ} although renormalized in temperature [142, 58], never reaches the limit $K_{\rho} = 0$. A value $K_{\rho} \approx 0.1 - 0.2$ would be consistent with ambient pressure NMR data in (TMTSF)₂PF₆ at $T \gtrsim 50$ K. Similar figures for K_{ρ} have been suggested in (TMTSF)₂ClO₄ (or (TMTSF)₂PF₆ under pressure) [51, 143], although the influence of interchain

coupling in that region is probably not small and should contribute to some extent to the relaxation rate.

As shown in Fig. 12, another regime of relaxation is reached at very low temperature ($T < 8$ K), where a behavior $1/T_1 \propto T$ is recovered [51, 69, 70, 144]. The low temperature regime looks like a Korringa law with an enhancement factor of the order 10 with respect to the regime $T > 30$ K. It has been first proposed that this change in behavior for the enhancement originates in the dimensionality crossover of one-particle coherence and the restoration of a Fermi liquid component in two directions. It is still an open problem to decide whether the Fermi liquid properties recovered below 8 K are those of a 2-D or 3-D electron gas. Furthermore the intermediate temperature regime $8 \text{ K} \lesssim T \lesssim 80 \text{ K}$ requires an improvement of the theory taking into account all transient effects due to interchain coupling.

The Wilson ratio in a Luttinger liquid.— The Fermi liquid which is recovered below 8 K is not following the canonical behavior as shown by its response to a magnetic field. According to high-field NMR studies of ⁷⁷Se in (TMTSF)₂ClO₄ [74], the uniform spin susceptibility – as obtained from the Knight shift – is found to be insensitive to the application of a magnetic field up to 15 T along c^* . As already discussed in Section 3, the Sommerfeld constant of the electronic specific heat shows an important field dependence [62], which cannot be explained with the Fermi liquid model (Figure 10). The Luttinger liquid scenario, however, offers an interesting avenue to understand these features if one considers this experimental finding as reminiscent of the expected behavior in a slightly doped Mott insulator as the metal-insulator transition is approached (i.e. band filling approaching half-filling). The Wilson ratio in a Luttinger liquid reads [145] :

$$R_W = \frac{2v_{\rho}}{v_{\rho} + v_{\sigma}},$$

in terms of charge and spin velocities. Therefore, R_W decreases as the Mott insulating regime is approached since according to (42), $v_{\rho} \rightarrow 0$, while the spin part – which is independent of the Umklapp scattering – is not sensitive to the proximity of the Mott insulator. The behavior of the Wilson ratio under magnetic field provides another example of marginal Fermi liquid character in 2-D anisotropic conductor at low temperature and suggests that the spin and charge separate as a result the electronic confinement induced by a magnetic field [32].

One-particle spectral properties of a Luttinger liquid.— The absence of quasi-particles in a Luttinger liquid is also manifest in the one-particle spectral properties. As we have seen in the framework of the 1D renormalization group method in the gapless case, there is a power-law decay of the one-particle spectral weight at the Fermi level. This power law behavior is also confirmed in the framework of the bosonization technique [146, 147], namely

$$A_p(k_F^0, \omega) \sim |\omega|^{\alpha-1}, \quad (49)$$

where $\alpha = \frac{1}{4}(K_\rho + 1/K_\rho - 2)$. A power law is also found for the density of states

$$N(\omega) = \sum_p \int A_p(k_F^0, \omega) dk \sim |\omega|^\alpha. \quad (50)$$

Thus as soon as right and left-moving carriers interact with each other, $K_\rho < 1$ so that $\alpha > 0$, which leads to a dip in the density of states at the Fermi level. As a function of temperature, one can replace ω by T and the density of states vanishes as a power of the temperature.

When Umklapp processes are relevant, K_ρ decreases and α increases at low energy leading to a pronounced depression of the spectral weight near k_F^0 . Within a one-dimensional scenario for the normal phase in the Bechgaard salts, this situation is of practical interest. Experimentally both ARPES [99] and integrated photoemission [100] signals fail to detect any quasi-particle states in systems like $(\text{TMTSF})_2\text{ClO}_4$ and $(\text{TMTSF})_2\text{PF}_6$ (Figure 20); instead, a quite pronounced reduction of the spectral weight is found, which one would be tempted to describe using the above expressions with a sizable value of $\alpha \simeq 1.5$ ($K_\rho \simeq 1/8$); a value which we may add congruent with those extracted from a low-dimensional description of NMR [58], optical data [148] (see below), and DC transport [81]. Although photoemission results call into question the viability of the Fermi liquid description in these systems, they confront us, however, with many difficulties that do not conform with the prediction of the one-dimensional theory. Among them, the absence of dispersing structure and a power-law frequency dependence that is spreaded out over a large energy scale of the order of 1 eV, may indicate that surface effects should be taken into account in the interpretation.

ARPES experiments have also been carried out in the insulating sulfur compound $(\text{TMTTF})_2\text{PF}_6$ (Figure 20) and as expected [149], the charge gap is clearly seen as an energy shift of ~ 100 meV in the spectral weight, a value that agrees with DC and optical transport.

Transverse and optical transport.— Transport properties along directions transverse to the stacking axis can add to the understanding of this strange behavior [81]. If we consider the c direction which corresponds to the direction of weakest overlap, not much optical work has been devoted to this direction but the absence of any significant reflectance in the FIR regime for $(\text{TMTSF})_2\text{AsF}_6$ at $T = 30$ K has been attributed to the absence of coherent band transport along this direction down to (at least) 30 K in fair agreement with band calculations leading to $t_{\perp c} \approx 10 - 20$ K.

Extending the arguments proposed for the incoherent transverse transport developed in Q-1-D conductors to the 2-D conductors, one can infer as previously pointed out in Section 3 that σ_c is directly related to the physics of the $a-b$ planes and therefore could probe whether transport proceeds via collective modes or independent quasi-particles. The existence of maximum in ρ_c at T_m which evolves under pressure and reaches about 300 K at 10 kbar and the striking different temperature dependencies for the *in* and *out* of plane resistances suggest an interpretation in terms of a non-Fermi liquid approach at $T > T_m$. Assuming the $a-b$

planes can be described by an array of chains forming 1-D Luttinger liquids at $T > T_m$ the interplane transport can only proceed via the hopping of individual particles. For such a situation to occur a particle has to be rebuilt out of the Luttinger liquid by recombining its charge and spin components. The particle can then hop onto a neighboring stack, contributing to σ_c and then decay into the Luttinger liquid again. The transverse interplane conductivity has been derived theoretically when the physics of electrons in chains is governed by a 1-D Luttinger regime and becomes [81]:

$$\sigma_c(T) \approx t_{\perp c}^2 \frac{e^2}{\hbar} \frac{ac}{v_c^2} \left(\frac{T}{v_c}\right)^{2\alpha}, \quad (51)$$

where the exponent α enters the density of states near the Fermi energy which is proportional to $|\omega|^\alpha$, as we have seen above. Following this model, ρ_c should behave like $\rho_c(T) \approx T^{-2\alpha}$ in the Luttinger liquid domain with α positive and ranging from infinity in a Mott insulator to zero in a non-interacting Fermi liquid.

If one reverts to the constant volume data of Figure 15, a law such as $\rho_c(T) \approx T^{-1.4}$ fits the data fairly well above T_m , i.e. $\alpha = 0.7$. Below 60 K, there is hardly any difference between constant T and constant P variations since the thermal expansion is there greatly suppressed. As for the longitudinal transport, the result is displayed in Fig. 14, where a cross-over from a superlinear to a linear (or sublinear) power law temperature dependence is observed in the vicinity of 80 K. Fig. 15 emphasizes the remarkable feature of $(\text{TMTSF})_2\text{PF}_6$, namely, opposite temperature dependencies for interplane and chain resistivities above T_m .

We shall see below that the transport properties above T_m are consistent with the picture of Luttinger chains in $(a-b)$ planes. The exponent $\alpha = 0.7$ derived from the constant volume transverse data leads to $K_\rho = 0.22$. This value of K_ρ allows in turn a prediction for the constant volume T -dependence for ρ_a . The only scattering process through which electron-electron collisions can contribute to resistivity in this 1-D electron gas occurs when the total momentum transfer is commensurate with a Brillouin zone wave vector. For the situation of a 1/4-filled 1-D band which is likely to apply to $(\text{TMTSF})_2\text{PF}_6$ as the dimerization can be forgotten in first approximation ($\Delta_D < t_{\perp b}$), the resistivity due to 1/4-filled Umklapp becomes [96]:

$$\rho_a(T) \approx g_{1/4}^2 T^{16K_\rho - 3}. \quad (52)$$

A value $K_\rho = 0.22$ would in turn lead to $\rho_a(T) \approx T^{0.52}$ which is in qualitative agreement with the sublinear T -dependence in Fig. 14, given the degree of arbitrariness which underlies the conversion procedure.

The temperature T_m signals the beginning of a cross-over between a high temperature Luttinger regime for the chains along a and a 2-D regime where the system leaves progressively the LL physics before recovering the canonical 2-D Fermi liquid regime only around 10 K (Figure 5).

Several experimental results show that the intermediate regime $10 \text{ K} < T < T_m$ behaves as a very unusual anisotropic 2-D metal. As revealed by optical data in all Se-based salts, there still exists at $T = 20$ K a clear-cut gap in the frequency dependence of the conductivity, $2\Delta_\rho \approx 200 \text{ cm}^{-1}$ [93].

This semiconducting-like spectrum contains 99% of the oscillator strength and the large DC conductivity is provided

by a very narrow zero frequency mode carrying the 1% left over. As the spin susceptibility remains finite in the same T -regime only 30-40% below its value at 300 K, the FIR gap in conductivity provides a remarkable illustration for the spin-charge separation which still prevails although the longitudinal DC transport looks like that of a Fermi liquid.

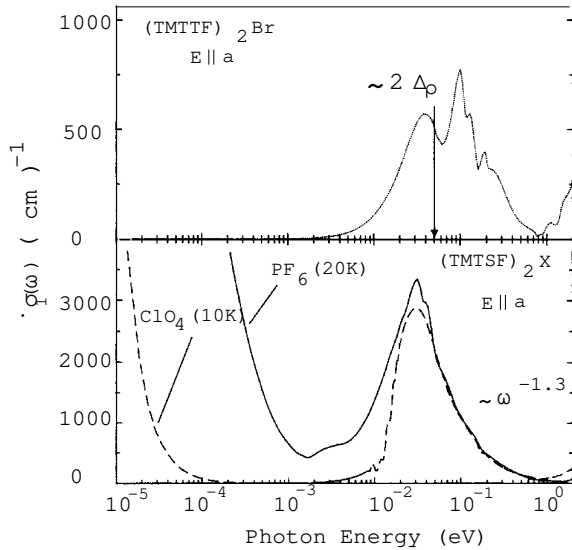


Figure 26: One-chain optical conductivity of members of the $(\text{TM})_2\text{X}$ series in the normal phase at low temperature. The arrow indicates location of the gap observed via the dielectric response in the case of $(\text{TMTTF})_2\text{Br}$, after [93].

As the temperature is decreased below T_m , the anisotropy ratio ρ_c/ρ_a remains temperature dependent, a feature that can be hardly tied with a Fermi liquid picture. It is only below 10 K in $(\text{TMTSF})_2\text{PF}_6$ under 9 kbar that the ratio becomes constant in temperature suggesting a recovery of the usual Fermi liquid behavior (Figure 16).

It is also interesting to notice that the existence of a T_m marking the border between a high temperature Luttinger liquid and a 2D non-Fermi-liquid can be also extended to $(\text{TMTTF})_2\text{PF}_6$ under pressure (Fig. 5). Furthermore T_m shows a very large pressure coefficient. This property clearly rules out a simple relation such as $T_m \approx t_{\perp b}$ which is expected for the 2-D cross-over of non-interacting electrons since $\delta \ln t_{\perp b}/\delta P \approx +2\% \text{ kbar}^{-1}$ from the theory whereas $\delta \ln T_m/\delta P \approx +20\% \text{ kbar}^{-1}$ in $(\text{TMTSF})_2\text{PF}_6$ under ambient pressure. This feature suggests that the beginning of the cross-over towards a 2D-NFL regime is renormalized by the intra-chain interactions.

The power law coefficient can also be derived from the optical response at frequencies ω greater than the Hubbard gap since then the frequency dependent conductivity is governed by inter Hubbard sub-band transitions and becomes $\sigma(\omega) \approx \omega^{4n^2 K_\rho - 5}$ (with $n = 2$ for the quarter-filled situation). This is markedly different from the behavior of the conductivity expected through the gap of a regular semiconductor where $\sigma(\omega) \approx \omega^{-3}$. The experimental data of Figure 26 for $(\text{TMTSF})_2\text{PF}_6$ and ClO_4 both give the exponent -1.3 in the power law frequency dependence in the low

temperature range (10–20 K) of the 2D intermediate phase. This exponent leads to $K_\rho = 0.23$ in case of a quarter-filled 1-D band [96].

5. Conclusion

This article aimed at surveying the physics of $(\text{TM})_2\text{X}$ conductors in the high temperature regime, *i.e.* in a regime too high in temperature for 3-D long range order (structural, magnetic or superconducting) to become stable.

We have shown a remarkable evolution throughout these Q-1-D conductors with commensurate band-filling from Mott localized systems with a significant charge gap $2\Delta_\rho \approx 1000 - 2000 \text{ cm}^{-1}$ in $(\text{TMTTF})_2\text{X}$ making the finite inter-chain kinetic coupling irrelevant at low temperature all the way to the selenium-based conductors displaying a metallic-like behavior as far as the longitudinal DC transport is concerned. However, a wealth of properties suggest that the $(\text{TMTSF})_2\text{X}$ conducting salts cannot be viewed as canonical Fermi-liquid-like conductors. Transverse (along c^*) and longitudinal resistivities exhibit opposite temperature dependencies above a temperature marking the progressive establishment of a transverse coherence between chains in the $(a-b)$ planes. Even below that cross-over temperature (which is $\approx 80 \text{ K}$ in $(\text{TMTSF})_2\text{PF}_6$ at ambient pressure) remnants of a non-Fermi behavior are the highlights of these materials. A gap in the charge sector ($2\Delta_\rho \approx 200 \text{ cm}^{-1}$) co-existing with a DC conducting mode carrying only a minor fraction of the overall spectral weight and far too narrow to be understood in terms of a classical Drude model. These features suggest that the large conductivity of $(\text{TMTSF})_2\text{X}$ salts developing at low temperature could possibly be ascribed to the existence of the finite interchain coupling acting as an actual dopant in these otherwise commensurate Mott insulating materials. In spite of some similarities, in the behavior of their transport properties, $(\text{TMTSF})_2\text{X}$ and the anisotropic ruthenates, Sr_2RuO_4 [150], are likely to be very different since it is believed that the latter conductor exhibits a coherent to incoherent transition along the c^* axis around 100 K while the c^* transport remains incoherent in $(\text{TMTSF})_2\text{PF}_6$ down to low temperature even though ρ_{c^*} behaves metal-like versus temperature.

Moving towards the low temperature regime, the concept of quasiparticle is recovered *albeit* with a severe renormalization as illustrated by the factor ≈ 10 enhancement measured in the low energy spin sector via the nuclear spin-lattice relaxation rate of $(\text{TMTSF})_2\text{ClO}_4$ at ambient pressure or $(\text{TMTSF})_2\text{PF}_6$ under pressure below 8 K [58]. It is the Fermi nature of the 2-D electron gas which is responsible for the suppression of an itinerant antiferromagnetic ground state in $(\text{TMTSF})_2\text{PF}_6$ under pressure. Furthermore, a mean-field theory based on a 2-D Fermi electron gas has also been extremely successful in the low temperature domain explaining the restoration of a sequence of ground states under a magnetic field exhibiting a non-commensurate magnetic modulation. [103, 104]. The successful description of this cascade of field-induced phases in terms of ‘BCS quasiparticles’ is a bit puzzling, however, if one considers that the normal phase under magnetic field can be hardly tied in the Fermi liquid picture. The restoration of quasi-particles following the occurrence of long-range order is not specific

to the Bechgaard salts, it indeed finds a large echo in the context of high- T_c cuprate superconductors for which quasi-particles ‘à la BCS’ are known to emerge in the superconducting state in spite of the fact that the normal state does not fit at all with a Fermi liquid description [151, 152]. Not less puzzling is a certain class of angular dependent magnetotransport experiments performed at very low temperature in $(\text{TMTSF})_2\text{X}$ [153, 35]. These can be fittingly described by a classical Boltzmann theory which supports the recovery of coherent quasi-particles whose energy spectrum apparently shows no corrections due to many-body effects. This again occurs in contradiction with many anomalous properties that show marginal part played by quasi-particles in a sizable part of the normal phase at high temperature. The theoretical frame that would solve this paradox is not known so far.

The various ground states that are encountered in the $(\text{TM})_2\text{X}$ series have not been overviewed in the present survey. To make a long story short let us mention that $(\text{TMTTF})_2\text{PF}_6$ displays a classical example for the spin-Peierls transition at $T_{\text{SP}} = 18$ K from a 1-D Mott insulator to a spin singlet ground state accompanied by a lattice dimerization [132]. The spin-Peierls state turns into a commensurate Néel antiferromagnet under a pressure of about 8 kbar (Fig. 5) [154, 155]. A recent detailed NMR under pressure study displays a phase diagram in the vicinity of the critical pressure showing a competition between two order parameters resulting in the suppression of the ordering temperature and the possible existence of a quantum critical point [156]. Increasing high pressure, the 1-D localization at high temperature is no longer efficient as the cross-over temperature T_m seen in ρ_c rises under pressure from around 13 kbar. The Néel antiferromagnet turns into a SDW insulating state [157, 141]. Recent very high pressure data [158] reveal a sharp suppression of the SDW phase transition above 40 kbar and the superconducting phase similar to what has been observed in $(\text{TMTSF})_2\text{PF}_6$ at 9 kbar is expected to become stable above 44 kbar or so.

The superconducting phase of 1-D organic conductors has not yet been intensively studied unlike the superconducting phase of 2-D organic conductors. Even if theoretical predictions [159] support the existence of an exotic pairing via the interchain exchange of antiferromagnetic fluctuations experimental evidences are still scars. It has been known for a long time that the sensitivity of the superconducting transition to defects is much higher than what can be expected in a regular superconductor [160, 161]. A recent thermal conductivity study of the superconducting state of $(\text{TMTSF})_2\text{ClO}_4$ [162] has shown that the superconducting order parameter cannot have nodes on the 1-D open Fermi surface. This finding still leaves open various exotic scenarios: a spin-triplet pairing with the possibility of reentrant superconductivity at very high magnetic fields aligned along the b' direction [163, 164, 165] or even d-wave pairing for $(\text{TMTSF})_2\text{ClO}_4$ in the presence of anion ordering at low temperature. There is still a lot more work to be done on the superconducting phase of 1-D organic superconductors. The SDW ground state of say, $(\text{TMTSF})_2\text{PF}_6$ has also been the subject of an intense effort [166, 167, 168, 169, 170]. The whole condensate pinned by impurities can be put into

motion by an electric field larger than threshold fields of order 2 mV/cm [171] (instead of 100 mV/cm for CDW condensates) and gives rise to a collective conduction channel. The systematic study of the SDW sliding conductivity [172] and the frequency dependence of the dielectric constant in a $(\text{TM})_2\text{X}$ alloy series [173] has shown the existence of two different channels of phason damping; one is due to the dissipation of quasi-particles while the other one is related to the presence of defects. Furthermore, the non-commensurate nature of the density wave goes hand in hand with its large polarizability and a dielectric constant higher than 10^{19} [174]. We are aware that this article does not exhaust all properties of these fascinating materials, however we consider that understanding in details their normal phase properties could also be of significant help for the closely related systems such as the cuprate spin-ladder 1-D conductors which display superconductivity under pressure [175], although still in the presence of low lying spin excitations [176].

As we were finishing this article, H.J. Schulz passed away. It is the loss of a colleague for the whole physics community and for both of us in particular since Heinz has been a remarkable friend, active and productive in the domain of low dimensional fermiology over the past 20 years.

References

- [1] G. Hardy and J. Hulm, *Phys. Rev.* **87**, 884 (1953).
- [2] B. Matthias, T. Geballe, S. Geller, and E. Corenwitz, *Phys. Rev.* **95**, 1435 (1954).
- [3] J. Hulm and B. Matthias, *Science* **208**, 881 (1980).
- [4] F. Steglich *et al.*, *Phys. Rev. Lett.* **43**, 1892 (1979).
- [5] J. Bednorz and K. Müller, *Z. Phys. B* **64**, 189 (1986).
- [6] W. Little, *Phys. Rev.* **134A**, 1416 (1964).
- [7] J. Bardeen, L. Cooper, and J. Schrieffer, *Phys. Rev.* **108**, 1175 (1957).
- [8] H. Akamatsu, H. Inokuchi, and Y. Matsunaga, *Nature* **173**, 168 (1954).
- [9] L. Coleman *et al.*, *Solid State Comm.* **12**, 1125 (1973).
- [10] J. Ferraris, D. Cowan, V. Walatka, and J. Perlstein, *J. Am. Chem. Soc.* **95**, 948 (1973).
- [11] D. Schäfer *et al.*, *Solid State Comm.* **14**, 347 (1974).
- [12] R. Groff, A. Suna, and R. Merrifield, *Phys. Rev. Lett.* **33**, 418 (1974).
- [13] F. Denoyer, R. Comès, A. Garito, and A. Heeger, *Phys. Rev. Lett.* **35**, 445 (1975).
- [14] R. Peierls, *Quantum Theory of Solids* (Oxford University Press, London, 1955), p.108.
- [15] B. Horovitz, H. Gutfreund, and M. Weger, *Phys. Rev. B* **12**, 3174 (1975).
- [16] D. Jérôme and H. Schulz, *Adv. in Physics* **31**, 299 (1982).
- [17] R. H. Friend, M. Miljak, and D. Jérôme, *Phys. Rev. Lett.* **40**, 1048 (1978).
- [18] S. Megtert *et al.*, *Solid State Commun.* **31**, 977 (1979).
- [19] C. Jacobsen, K. Mortensen, J. Andersen, and K. Bechgaard, *Phys. Rev. B* **18**, 905 (1978).
- [20] A. Andrieux, C. Durouère, D. Jérôme, and K. Bechgaard, *J. Phys. (Paris) Lett.* **40**, 381 (1979).
- [21] J. Pouget, *Chemica Scripta* **55**, 85 (1981).
- [22] K. Bechgaard *et al.*, *Solid State Comm.* **33**, 1119 (1980).
- [23] J. Galigne *et al.*, *Acta Cryst.* **B 35**, 2609 (1979).
- [24] G. Brun *et al.*, *C.R. Acad. Sc. (Paris)* **284 C**, 211 (1977).

- [25] C. Coulon *et al.*, J. Phys. (Paris) **43**, 1059 (1982).
- [26] D. Jérôme, Science **252**, 1509 (1991).
- [27] F. D. M. Haldane, J. Phys. C **14**, 2585 (1981).
- [28] C. Bourbonnais and D. Jérôme, Science **281**, 1156 (1998).
- [29] L. Gor'kov, J. Phys. I (France) **6**, 1697 (1996).
- [30] D. Jérôme, A. Mazaud, M. Ribault, and K. Bechgaard, J. Phys. (Paris) Lett. **41**, L95 (1980).
- [31] D. G. Clarke *et al.*, Science **229**, 2071 (1998).
- [32] K. Behnia *et al.*, Phys. Rev. Lett. **74**, 5272 (1995).
- [33] D. G. Clarke and S. Strong, Adv. Phys. **46**, 545 (1997).
- [34] V. Yakovenko, preprint Cond-matter/9802172 (unpublished).
- [35] I. J. Lee and M. J. Naughton, Phys. Rev. B **58**, R13 343 (1998).
- [36] V. Ilakovac *et al.*, Phys. Rev. B **50**, 7136 (1994).
- [37] P. M. Grant, J. Phys. (Paris) Coll. **44**, 847 (1983).
- [38] K. Yamaji, J. Phys. Soc. of Japan **51**, 2787 (1982).
- [39] L. Ducasse *et al.*, J. Phys. C **39**, 3805 (1986).
- [40] L. Balicas *et al.*, J. Phys. I (France) **4**, 1539 (1994).
- [41] R. Moret, J. P. Pouget, R. Comes, and K. Bechgaard, J. Phys. (France) **46**, 1521 (1985).
- [42] J. P. Pouget and S. Ravy, J. Phys. I (France) **6**, 1501 (1996).
- [43] M. J. Naughton *et al.*, Phys. Rev. Lett. **61**, 621 (1995).
- [44] S. K. McKernan *et al.*, Phys. Rev. Lett. **75**, 1630 (1995).
- [45] W. Kang, S. T. Hannahs, and P. M. Chaikin, Phys. Rev. Lett. **70**, 3091 (1993).
- [46] E. Hanson *et al.*, proc. of ICSM'98 (unpublished).
- [47] A. G. Lebed, J. Phys. I (France) **6**, 1819 (1996), and references therein.
- [48] R. Moret *et al.*, Phys. Rev. Lett. **57**, 1915 (1986).
- [49] F. Wudl, D. Naleveck, J. M. Torup, and N. W. Extine, Science **22**, 415 (1983).
- [50] V. J. Emery, J. Phys. (Paris) Coll. **44**, C3 (1983).
- [51] C. Bourbonnais *et al.*, J. Phys. (Paris) Lett. **45**, L755 (1984).
- [52] D. Pines and P. Nozières, *The Theory of Quantum Liquids: Normal Fermi Liquids* (Benjamin, New York, 1966).
- [53] N. Miljak, J. R. Cooper, and K. Bechgaard, J. Phys. Coll. **44**, 893 (1983).
- [54] N. Miljak and J. R. Cooper, Mol. Cryst. Liq. Cryst. **119**, 141 (1985).
- [55] C. S. Jacobsen, J. Phys. C **19**, 5643 (1986).
- [56] A. Fritsch and L. Ducasse, J. Phys. I (France) **1**, 855 (1991).
- [57] F. Castet, A. Fritsch, and L. Ducasse, J. Phys. I (France) **6**, 583 (1996).
- [58] P. Wzietek *et al.*, J. Phys. I (France) **3**, 171 (1993).
- [59] F. Mila and K. Penc, Phys. Rev. B **51**, 1997 (1995).
- [60] K. G. Wilson, Rev. Mod. Phys. **47**, 773 (1975).
- [61] P. Garoche, R. Brusetti, and K. Bechgaard, Phys. Rev. Lett. **49**, 1346 (1982).
- [62] R. Brusetti, P. Garoche, and K. Bechgaard, J. Phys. C **16**, 2495 (1983).
- [63] F. Pesty, P. Garoche, and K. Bechgaard, Phys. Rev. Lett. **55**, 2495 (1985).
- [64] L. P. Gor'kov, Europhys. Lett. **31**, 49 (1995).
- [65] J. Moriya, J. Phys. Soc. Jpn. **18**, 516 (1963).
- [66] G. Soda *et al.*, J. Phys. (Paris) **38**, 931 (1977).
- [67] C. Bourbonnais *et al.*, Phys. Rev. Lett. **62**, 1532 (1989).
- [68] C. Bourbonnais, J. Phys. I (France) **3**, 143 (1993).
- [69] T. Takahashi, D. Jérôme, and K. Bechgaard, J. Phys. (Paris) **45**, 945 (1984).
- [70] M. Takigawa and G. Saito, J. Phys. Soc. Jpn **55**, 1233 (1986).
- [71] F. Devreux and M. Nechtchein, in *Proc. of the International Conference of Quasi-One-Dimensional Conductors I*, Edited by S. Barisic, A. Bjelis, J. R. Cooper and B. Leontic (Springer, Lectures Notes in Physics, Vol. 95, New York, 1978), p. 145.
- [72] C. Bourbonnais *et al.*, Europhys. Lett. **6**, 177 (1988).
- [73] L. J. Azevedo, J. E. Schirber, and J. C. Scott, Phys. Rev. Lett. **49**, 826 (1982).
- [74] P. Caretta *et al.*, in *Proc. of the Int. Conference on High Magnetic Field Phenomena-II Talahassee* (World Scientific, New Jersey, 1995), p. 328.
- [75] L. P. Gorkov and M. Mochena, Phys. Rev. B **57**, 6204 (1998).
- [76] B. Welber, P. Seiden, and P. Grant, Phys. Rev. B **18**, 2692 (1987).
- [77] S. Megtert *et al.*, Solid State Comm. **37**, 875 (1981).
- [78] P. Auban-Senzier (unpublished).
- [79] B. Gallois, Ph.D. thesis, Univ. Bordeaux I, 1987.
- [80] C. S. Jacobsen, K. Mortensen, M. Weger, and K. Bechgaard, Solid State Commun. **38**, 423 (1981).
- [81] J. Moser *et al.*, Eur. Phys. J. B **1**, 39 (1998).
- [82] P. Fertey, M. Poirier, and P. Batail, proc. of ICSM'98 (unpublished).
- [83] L. Balicas and D. Jerome (unpublished).
- [84] S. E. Brown *et al.*, Synthetic Metals **86**, 1937 (1997).
- [85] R. Laversanne *et al.*, J. Phys. (Paris) Lett. **45**, L393 (1984).
- [86] C. S. Jacobsen, D. Tanner, and K. Bechgaard, Phys. Rev. Lett. **46**, 1142 (1981).
- [87] C. S. Jacobsen, D. Tanner, and K. Bechgaard, Mol. Cryst. Liq. Cryst. **79**, 261 (1982).
- [88] C. Jacobsen, D. Tanner, and K. Bechgaard, Phys. Rev. B **28**, 7019 (1983).
- [89] J. F. Kwak, Phys. Rev. B **26**, 4789 (1982).
- [90] T. Ishiguro and K. Yamaji, *Organic Superconductors*, Vol. 88 of *Springer-Verlag Series in Solid-State Science* (Springer-Verlag, Berlin, Heidelberg, 1990).
- [91] C. Bourbonnais, in *Les Houches, Session LVI (1991), Strongly interacting fermions and high- T_c superconductivity*, edited by B. Doucot and J. Zinn-Justin (Elsevier Science, Amsterdam, 1995), p. 307.
- [92] Y. Suzumura, M. Tsuchiizu, and G. Grüner, Phys. Rev. B **57**, R15 040 (1998).
- [93] V. Vescoli *et al.*, Science **281**, 1181 (1998).
- [94] N. Cao, T. Timusk, and K. Bechgaard, J. Phys. I (France) **6**, 1719 (1996).
- [95] M. Dressel *et al.*, Phys. Rev. Lett. **77**, 398 (1996).
- [96] T. Giamarchi, Physica **B230-232**, 975 (1997).
- [97] J. Favand and F. Mila, Phys. Rev. B **54**, 10 425 (1996).
- [98] D. Pedron, R. Bozio, M. Meneghetti, and C. Pecile, Phys. Rev. B **49**, 10 893 (1994).
- [99] F. Zwick *et al.*, Phys. Rev. Lett. **79**, 3982 (1997).
- [100] B. Dardel *et al.*, Europhys. Lett. **24**, 687 (1993).
- [101] C. Seidel and V. N. Prigodin, J. Phys. (Paris) Lett. **44**, L403 (1983).
- [102] P. Chaikin, J. Phys. I (France) **6**, 1875 (1996).
- [103] L. P. Gorkov and A. G. Lebed, J. Phys. (Paris) Lett. **45**, L433 (1984).
- [104] M. Héritier, G. Montambaux, and P. Lederer, J. Phys. (Paris) Lett. **45**, L943 (1984).
- [105] K. Yamaji, Synthetic Metals **13**, 19 (1986).

- [106] L. Chen, K. Maki, and V. Virosztek, *Physica* **143B**, 444 (1986).
- [107] I. E. Dzyaloshinskii and A. I. Larkin, *Sov. Phys. JETP* **34**, 422 (1972).
- [108] Y. A. Bychkov, L. P. Gorkov, and I. Dzyaloshinskii, *Sov. Phys. JETP* **23**, 489 (1966).
- [109] J. Solyom, *Adv. Phys.* **28**, 201 (1979).
- [110] S. Barisic, *J. Phys. (Paris)* **44**, 185 (1983).
- [111] S. Botric and S. Barisic, *J. Phys. (Paris)* **45**, 185 (1984).
- [112] S. Barisic, *Mol. Cryst. Liq. Cryst.* **119**, 413 (1985).
- [113] S. Barisic and S. Brazovskii, in *Recent Developments in Condensed Matter Physics*, edited by J. T. Devreese (Plenum, New York, 1981), Vol. 1, p. 327.
- [114] K. Penc and F. Mila, *Phys. Rev. B* **50**, 11 429 (1994).
- [115] V. J. Emery, B. R., and S. Barisic, *Phys. Rev. Lett.* **48**, 1039 (1982).
- [116] F. Mila, *Phys. Rev. B* **52**, 4788 (1995).
- [117] F. Mila and K. Penc (unpublished).
- [118] C. Bourbonnais and L. G. Caron, *Int. J. Mod. Phys. B* **5**, 1033 (1991).
- [119] E. Lieb and F. Y. Wu, *Phys. Rev. Lett.* **20**, 1445 (1968).
- [120] M. Kimura, *Prog. Theor. Phys.* **63**, 955 (1975).
- [121] L. P. Gor'kov and I. E. Dzyaloshinskii, *JETP Lett.* **18**, 401 (1973).
- [122] S. Brazovskii and Y. Yakovenko, *Sov. Phys. JETP* **62**, 1340 (1985).
- [123] C. Bourbonnais and L. G. Caron, *Physica* **143B**, 450 (1986).
- [124] T. Giamarchi, *Phys. Rev. B* **44**, 2905 (1991).
- [125] H. Shiba, *Phys. Rev. B* **6**, 930 (1972).
- [126] A. Maaroufi *et al.*, *J. Phys. (Paris) Coll.* **44**, 1091 (1983).
- [127] S. Parkin, J. C. Scott, J. B. Torrance, and E. Engler, *J. Phys. (Paris) Coll.* **44**, 1111 (1983).
- [128] J. Voit, *Rep. Prog. Phys.* **58**, 977 (1995).
- [129] H. J. Schulz, *Phys. Rev. Lett.* **64**, 2831 (1990).
- [130] F. Mila and X. Zotos, *Europhys. Lett.* **24**, 133 (1993).
- [131] E. Tutis and S. Barisić, *Phys. Rev. B* **42**, 1015 (1990).
- [132] J. Pouget *et al.*, *Mol. Cryst. Liq. Cryst.* **79**, 129 (1982).
- [133] J. P. Pouget and S. Ravy, *Synthetic Metals* **85**, 1523 (1997).
- [134] J. P. Pouget *et al.*, *Phys. Rev. Lett.* **37**, 437 (1976).
- [135] R. Comès, M. Lambert, H. Launois, and H. R. Zeller, *Phys. Rev. B* **8**, 571 (1973).
- [136] H. J. Schulz, G. Cuniberti, and P. Pieri, *cond-mat/9807366* (unpublished).
- [137] A. Luther and V. J. Emery, *Phys. Rev. Lett.* **33**, 589 (1974).
- [138] V. J. Emery, in *Highly Conducting One-Dimensional Solids*, edited by J. T. Devreese, R. E. Evrard, and V. E. van Doren (Plenum Press, New York, 1979), p. 247.
- [139] B. Gotschy *et al.*, *J. Phys. I (France)* **2**, 677 (1992).
- [140] D. Jérôme, in *Organic Conductors*, edited by J. P. Farges (M. Dekker, New York, 1994), p. 405.
- [141] B. J. Klemme *et al.*, *Phys. Rev. Lett.* **75**, 2408 (1995).
- [142] C. Bourbonnais, in *Low dimensional conductors and Superconductors*, edited by D. Jérôme and L. Caron (Plenum, New York, 1987), p. 155, vol. 155.
- [143] F. Creuzet *et al.*, *Synthetic Metals* **19**, 277 (1987).
- [144] L. J. Azevedo, J. E. Schirber, R. L. Greene, and E. M. Engler, *Physica* **B108**, 183 (1981).
- [145] H. J. Schulz, *Int. J. Mod. Phys. B* **5**, 57 (1991).
- [146] J. Voit, *Phys. Rev. B* **47**, 6740 (1993).
- [147] V. Meden and K. Schönhammer, *Phys. Rev. B* **46**, 15753 (1992).
- [148] V. Vescoli *et al.*, *Science* **281**, 1181 (1998).
- [149] J. Voit, *Eur. Phys. J. B* **5**, 505 (1998).
- [150] Y. Maeno *et al.*, *Nature* **372**, 532 (1994).
- [151] Z. X. Shen and D. S. Desseau, *Phys. Rep.* **253**, 1 (1995).
- [152] J. C. Campuzano *et al.*, *Phys. Rev. B* **53**, R14 737 (1996).
- [153] G. M. Danner, W. Kang, and P. M. Chaikin, *Phys. Rev. Lett.* **72**, 3714 (1994).
- [154] F. Creuzet, D. Jérôme, and A. Moradpour, *Mol. Cryst. Liq. Cryst.* **119**, 297 (1985).
- [155] L. G. Caron *et al.*, *Synthetic Metals* **27B**, 123 (1988).
- [156] D. Chow *et al.*, *Phys. Rev. Lett.* **81**, 3984 (1998).
- [157] F. Creuzet *et al.*, *Synthetic Metals* **19**, 289 (1987).
- [158] J. Moser (unpublished).
- [159] C. Bourbonnais and L. Caron, *Europhys. Lett.* **5**, 209 (1988).
- [160] S. Bouffard *et al.*, *J. Phys. C* **15**, 295 (1982).
- [161] R. Greene *et al.*, *Mol. Cryst. Liq. Cryst.* **79**, 183 (1982).
- [162] S. Belin and K. Behnia, *Phys. Rev. Lett.* **79**, 2125 (1997).
- [163] A. Lebed and K. Yamaji, *Phys. Rev. Lett.* **80**, 2697 (1998).
- [164] N. Dupuis, G. Montambaux, and C. A. R. S. de Melo, *Phys. Rev. Lett.* **70**, 2613 (1993).
- [165] I. J. Lee, M. J. Naughton, G. M. Danner, and P. M. Chaikin, *Phys. Rev. Lett.* **78**, 3555 (1997).
- [166] D. Jérôme, in *Physics and Chemistry of Low-Dimensional Inorganic Compounds*, edited by M. G. C. Schlenker, J. Dumas and S. Smaalen (Plenum Press, New York, 1996), p. 141.
- [167] G. Grüner, *Rev. Mod. Phys.* **66**, 1 (1994).
- [168] T. T. Y. Maniwa, H. Kawamura, and G. Saito, *Physica* **143B**, 417 (1986).
- [169] J. L. Musfeldt, M. Poirier, P. Batail, and C. Lenoir, *Phys. Rev. B* **51**, 8347 (1995).
- [170] J. L. Musfeldt, M. Poirier, P. Batail, and C. Lenoir, *Phys. Rev. B* **52**, 15983 (1995).
- [171] S. Tomic, J. Cooper, D. Jérôme, and K. Bechgaard, *Phys. Rev. Lett.* **62**, 462 (1989).
- [172] G. Kriza *et al.*, *Phys. Rev. Lett.* **66**, 1922 (1991).
- [173] O. Traetteberg *et al.*, *Phys. Rev. B* **49**, 409 (1994).
- [174] G. Mihaly, Y. Kim, and G. Grüner, *Phys. Rev. Lett.* **66**, 2806 (1991).
- [175] M. Uehara *et al.*, *J. Phys. Soc. Jpn.* **65**, 2764 (1996).
- [176] H. Mayaffre *et al.*, *Science* **279**, 345 (1998).